Creep Test on Fuel Cladding Tube for Fast Breeder Reactor (Fifth Program)

Dec., 1975

POWER REACTOR AND NUCLEAR FUEL DEVELOPMENT CORPORATION

NOT FOR PUBLICATION
TSN251 75-26
Oct., 1975

Creep Test on Fuel Cladding Tube for Fast Breeder Reactor (Fifth Program)*

Sadao Ohta*,** Isamu Ishiyama*,**
Masayuki Fujiwara*,** and
Hiroyuki Uchida**

Abstract

Elevated temperature tensile tests and uniaxial creep tests at 700 °C, and internal pressure creep rupture tests at 650 °C and 750 °C were performed on the fuel cladding tubes to be used in the core of the Japan Prototype Fast Breeder Reactor "MONJU" and the second core of the Japan Experimental Fast Breeder Reactor "JOYO".

Three kinds of fuel cladding tubes A, B, and C, made by two manufactures, were tested. Tubes B and C have larger grain size than tube A and tube C had rather higher nitrogen content than tubes A and B.

Results are summarized as follows:

1) The tensile properties of tubes A, B, and C were almost equivalent and satisfied the specification given by PNC.
2) Creep strength of tube B was higher than that of tube A.
3) Tube B showed longer creep rupture lives than tube A in the range of internal pressures applied at either test temperature. Creep rupture strength of tube C was equivalent to that of tube B at 750 °C.
4) There were significant differences between the creep and creep rupture properties of tube A and tubes B and C. It was thought that this was mainly attributed to the difference in grain size.

This is the translation of the report, SJ216 75-01, issued in July, 1975.

*Work performed by Kobe Steel, Ltd. under contract with Power Reactor and Nuclear Fuel Development Corp. (PNC).

**Kobe Steel, Ltd.

CONTENTS

1. Preface 1

2. Test Specimen 2

3. Test Method 7

3-1. High Temperature Tensile Tests 7

3-2. Uniaxial Creep Tests 8

3-3. Internal Pressure Creep Rupture Tests 8

3-4. Inspection of Test Specimen after Internal Pressure Creep Rupture Tests 11

4. Test Results 13

4-1. Results of High Temperature Tensile Tests 13

4-2. Results of Uniaxial Creep Tests 13

4-3. Results of Internal Pressure Creep Rupture Tests 13

4-4. Results of Inspection of Test Specimen after Internal Pressure Creep Rupture Tests 14

4-5. Discussion on the Difference in Creep Properties of A and B Materials 15

5. Conclusion 16

1. Preface

For the purpose of obtaining design data of FBR fuel elements, high temperature tensile test, uniaxial tensile creep test and internal pressure creep rupture test were performed on the secondary test-manufactured fuel cladding tube to be used in the core of "MONJU", the prototype FBR, and the newly manufactured fuel cladding tube to be used in the second core of "JOYO", the experimental FBR.

The present work involves the high temperature tensile test at 400 ~ 800 $^{\circ}C$, and the uniaxial tensile creep test (4 stress levels from 2 Kg/mm^2 to 12 Kg/mm^2 at 700 $^{\circ}C$) on the two kinds of materials (A and B) of the fuel cladding tube for "MONJU", and also the internal pressure creep rupture test on the three kinds of materials (A, B and C) for "JOYO MK-II" and one kind of material (C) for "MONJU" (up to the expected rupture time of 3,000 hrs.) These series of test are also accompanied by their metallographic tests.

2. Test Specimen

The materials, which were supplied by K and S companies for "MONJU" fuel cladding tube (18-8 Mo austenitic stainless steel, nominal measurement, 6.5^{ϕ} x 0.45^{t}_{mm}) and for "JOYO MK-II" fuel cladding tube (18-8 Mo austenitic stainless steel, nominal measurement 5.5^{ϕ} x 0.35^{t}_{mm}), were reprocessed at the Tokai Works, PNC into test pieces to be used for the present uniaxial creep tests and internal pressure creep rupture tests.

The configurations of these test pieces are shown in Figs. 1 and 2, and the test pieces for the uniaxial creep test are fitted to the testing machine with the screws on both ends, while those for the internal pressure creep rupture test are fitted to the test loop with the screw of the connecting conduit.

Tables 1 and 2 represent the mill sheets of the test specimens. The chemical composition hardly shows any difference among all the materials except that C-material indicates slightly higher N, and B and C-materials slightly exceeding in P.

Photos 1 ~ 3 represent the optical microstructure of the A, B and C materials. Tables 3 ~ 5 present the tabulation of hardness and grain size. There is noticed hardly any difference in hardness among the six kinds of cladding tube materials, but some difference in the degree of their grain size. B and C materials show considerably large γ grains size than in the case of A-material.

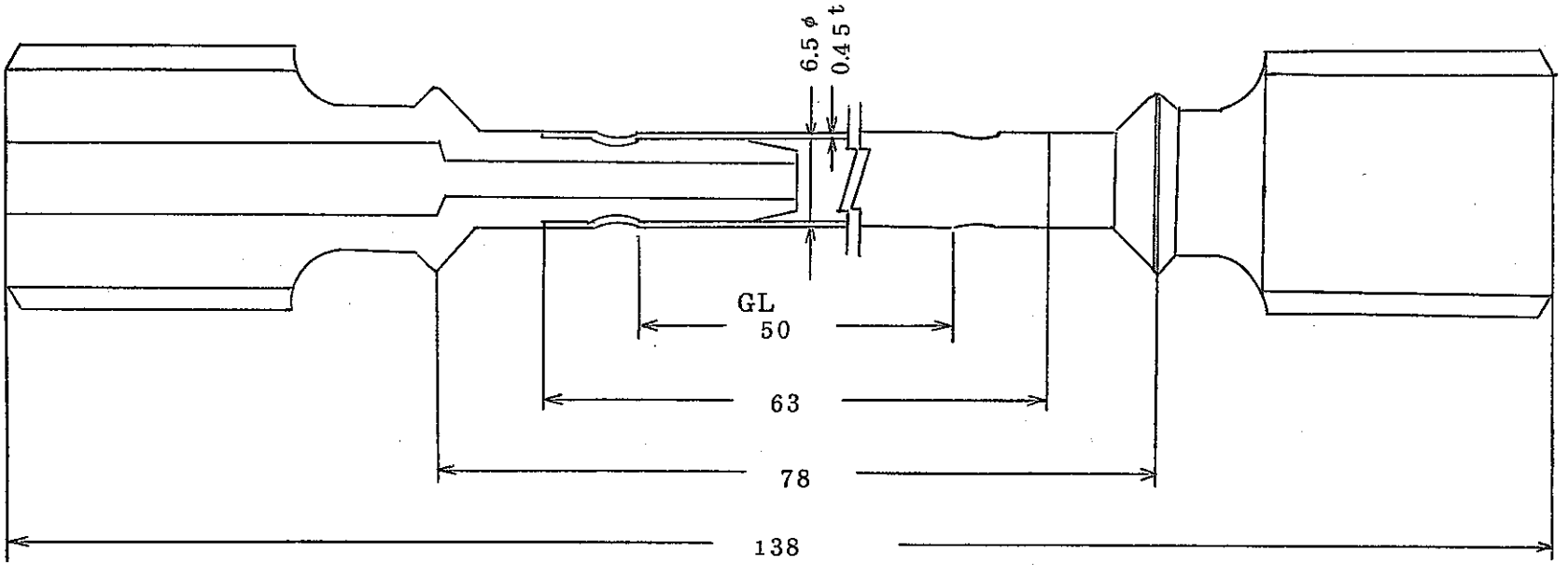

Fig. 1 Uniaxial Creep Test Piece

Scale 2/1.
Material for "MONJU"
Assembly Drawing

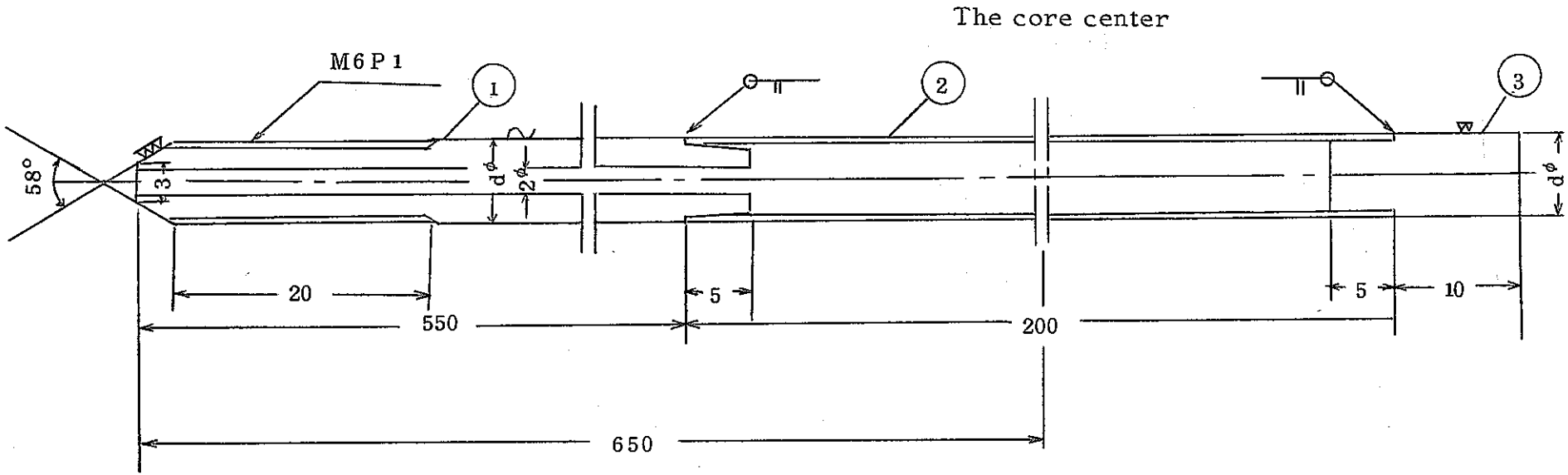

Cladding tube for MONJU" d=6.50 $^{\phi}$ mm

Cladding tube for "JOYO" d=5.50 $^{\phi}$ mm

End-plug	SUS 27
Cladding tube	SUS 32
Connecting conduit	SUS 27

Fig. 2 Internal Creep Rupture Test Piece

Table 1. Mill Sheet Showing Various Properties of Materials of "MONJU" Fuel Cladding Tube.

			A (K)		B (S)		C (S)	
			Charge № LO308 Mill Sheet № S-74.9		Heat № 380884 Mill Sheet № MS-RD-0003		Heat № 380700 Mill Sheet № MS-RD-0003	
Lot № (Tube №)			Lot 1 (3101～3350)		Lot 2(3224～3342)		Lot 1 (3001～3223)	
Annealing Temp. × Annealing time					1020℃ × 2min		1020℃ × 2min	
Cold Work			18 %		20 %		21 %	
			Ladle	Check	Ladle	Check	Ladle	Check
Chemical Composition (wt/%) Top of Ladle & Bottom of Ladle	C (0.035～0.064)		0.043 0.045	0.048 0.051	0.045 0.046	0.044 0.043	0.052 0.053	0.050 0.047
	Si (≦0.75)		0.65 0.66	0.67 0.67	0.51 0.51	0.51 0.52	0.52 0.50	0.50 0.51
	Mn (1.50～2.00)		1.64 1.67	1.66 1.65	1.75 1.75	1.82 1.82	1.79 1.79	1.86 1.84
	P (≦0.003)		0.010 0.011	0.011 0.011	0.022 0.022	0.021 0.022	0.021 0.022	0.022 0.022
	S (≦0.002)		0.005 0.005	0.005 0.005	0.005 0.006	0.006 0.006	0.008 0.009	0.008 0.008
	Ni (12.00～14.00)		13.69 13.81	13.90 13.87	12.86 12.93	13.04 12.96	12.81 12.80	12.82 12.79
	Cr (16.00～18.00)		17.50 17.44	17.44 17.48	16.80 16.80	16.90 17.05	17.20 17.05	16.75 16.75
	Mo (2.00～3.00)		2.27 2.28	2.30 2.25	2.44 2.46	2.51 2.52	2.50 2.50	2.50 2.52
	Co (≦0.10)		0.04 0.04	0.04 0.04	0.02 0.02	0.01 0.01	0.01 0.01	0.01 0.01
	B (≦0.00005)		0.0003 0.0003	0.0003 0.0003	0.0001 0.0001	0.0001 0.0001	0.0001 0.0001	0.0001 0.0001
	N (≦0.010)		0.005 0.006	0.0071 0.0070	0.0070 0.0072	0.0076 0.0076	0.0102 0.0105	0.0118 0.0118
Tensile Properties	Room Temperture	σ_B (Kg/mm²) (≧75)	85.6 85.7	85.5 85.0	83.1 82.0	81.9 81.8	82.9 84.6	85.4 84.7
		$\sigma_{0.2}$ (Kg/mm²) (≧60)	76.3 76.0	73.3 72.7	71.1 71.6	71.0 72.0	68.0 71.2	72.2 71.7
		ε (%) (≧10)	16 19	18 18	24 22	22 24	22 21	21 20
	650℃	σ_B (Kg/mm²) (≧40)	48.0 47.7	48.2 48.1	45.0 45.5	45.6 45.8	46.5 48.0	47.4 47.7
		$\sigma_{0.2}$ (Kg/mm²) (≧30)	45.8 45.3	46 45.8	39.8 41.0	40.6 40.2	41.3 41.2	42.4 41.4
		ε (%) (≧7)	12 14	13 14	25 20	21 22	18 16	13 20
Burst Properties		P_B (Kg/mm²) (≧1000)	1480 1460	1460 1470	1460 1470	1470 1430	1480 1510	1520 1530
		$P_{0.2}$ (Kg/mm²) (≧900)	1330 1320	1320 1320	1355 1370	1380 1340	1390 1400	1420 1440
Grain Size (≧6.0)			9.5	9.5	7.5		7.5	
Hardness (HV)			270	268	271	261	276	273

Table 2. Mill Sheet Showing Various Properties of Materials of "JOYO MK-Ⅱ" Fuel Cladding Tube

		A (K)		B (S)		C (S)	
		Charge № LO308 Mill Sheet № S-74-5		Heat № 380885 Mill Sheet № JS-RD-0002		Heat № 380705 Mill Sheat № JS-RD-0001	
Lot № (Tube №)		Lot 1 (0001～0250)		Lot 3 (0431～0750)		Lot 1 (0001～0264)	
Annealing Temp.×Annealing time				1020℃ × 2min		1020℃ × 2min	
Cold Work		17		20.0 ～ 21.0		21.0 ～ 21.2	
		Ladle	Check	Ladle	Check	Ladle	Check
Chemical Composition (wt%) Top of Ladle & Bottom of Ladle	C (0.035～0.064)	0.04 0.05	0.05 0.05	0.049 0.054	0.048 0.049	0.052 0.051	0.053 0.051
	Si (≦0.75)	0.65 0.66	0.70 0.70	0.52 0.52	0.51 0.50	0.50 0.51	0.53 0.53
	Mn (1.50～2.00)	1.64 1.67	1.67 1.63	1.73 1.73	1.51 1.53	1.84 1.83	1.78 1.77
	P (≦0.03)	0.010 0.011	0.011 0.011	0.022 0.022	0.020 0.020	0.021 0.021	0.022 0.021
	S (≦0.02)	0.005 0.005	0.005 0.005	0.007 0.007	0.009 0.009	0.007 0.007	0.007 0.008
	Ni (12.00～14.00)	13.69 13.81	13.66 13.71	12.82 12.84	12.90 12.94	12.88 12.92	12.92 12.92
	Cr (16.00～18.00)	17.50 17.44	17.54 17.46	16.85 16.75	17.05 17.00	17.50 17.10	17.20 17.10
	Mo (2.00～3.00)	2.27 2.28	2.26 2.27	2.42 2.42	2.50 2.56	2.50 2.50	2.48 2.50
	Co (≦0.10)	0.04 0.04	0.04 0.04	0.02 0.02	0.01 0.01	0.01 0.01	0.01 0.01
	B (≦0.0005)	0.0603 0.0003	0.0002 0.0003	0.0001 0.0001	0.0001 0.0001	0.0001 0.0001	0.0001 0.0001
	N (≦0.010)	0.005 0.006	0.0075 0.0071	0.0072 0.0074	0.0090 0.0086	0.0100 0.0104	0.0128 0.0128
Tensile Properties Room Temperature	σ_B (Kg/mm²) (≧75)	82.5 81.5	81.7 82.8	82.0 82.6	81.5 83.2	85.7 85.4	84.8 84.0
	$\sigma_{0.2}$ (Kg/mm²) (≧60)	73.0 71.2	71.3 73.0	69.8 70.3	69.2 70.4	76.2 75.7	70.7 69.7
	ε (%) (≧10)	24 24	22 22	19 19	18 20	17 17	19 20
Tensile Properties 650℃	σ_B (Kg/mm²) (≧40)	48.6 47.4	54.0 55.9	47.3 48.6	49.7 49.9	49.5 49.6	50.4 50.2
	$\sigma_{0.2}$ (Kg/mm²) (≧30)	39.1 41.8	44.6 45.7	42.6 43.3	42.9 43.3	44.2 44.9	43.5 43.3
	ε (%) (≧7)	19 17	14 13	17 15	15 13	15 17	16 14
Burst Properties	P_B (Kg/mm²) (≧1000)	1210 1220	1220 1220	1450 1470	1420 1420	1490 1480	1520 1480
	$P_{0.2}$ (Kg/mm²) (≧900)	1050 1060	1060 1050	1360 1370	1340 1340	1400 1400	1430 1400
Grain Size (≧6.0)		9.5	9.5	7.0	7.5	7.5	7.5
Hardness (HV)		265	255	268	268	290	284

3. Test Method

3-1 High Temperature Tesnsile Tests

The materials (A and B) for "MONJU" fuel cladding tube were exposed to a high temperature tensile test under the following conditions and test method:

(1) Test Pieces

$6.50^{\phi} \times 0.45^{t} \times 500^{l}$mm (GL = 50mm)

(2) Strain Rate

Against the 200mm of the soaking section of the heating furnace.

Up to yielding	0.3%/min.
After yield, deformed at	7.5%/min.
The total length of the heating furnace	410mm

(3) Test Temperature

The test was performed at 400, 500, 600, 700, 750 and 800 °C.

(4) Record

Up to yielding: Measured elongation by DTF, GL = 50mm, and recorded 200-time load-elongation curves.

After having yielded: Measured elongation by DTF the same as above, and recorded 4-time load elongation curves.

Test repeated on each material A and B under different conditions.

3-2 Uniaxial Creep Tests

The two kinds of materials A and B for "MONJU" fuel cladding tube were subjected to this uniaxial creep test. As illustrated by Fig. 1, the length of the test piece is 63mm and is partly reduced to prevent rupture from the welded section. The gauge length is 50mm between the end of reduced sections.

For this uniaxial creep test, four uniaxial creep testing machines were used by remodeling their loading method from the lever-type to the direct loading type with the maximum capacity 110 Kg.

For the heating device, a vertical tubular type heater with a SCR-type temperature regulator was employed. Its capacity was 2.5 Kw and the maximum heating temperature was 800 $^{\circ}C$.

The measurement of elongation was made by use of dialgauges (2 for one machine, with scaling of 0.001 mm) three times per day at appropriate intervals.

The test conditions are as follows:

Test temperature:	700 $^{\circ}C$
Test stress:	2, 4, 7, and 12 Kg/mm^2
Repetition:	One test piece for each of A and B materials under each changed condition.

3-3 Internal Pressure Creep Rupture Tests

This test was applied to the materials A, B and C for "JOYO MK-II" fuel cladding tube and material C for "MONJU" fuel cladding tube.

Fig. 3 represents the schematic diagram of the internal pressure creep testing equipment. The hydraulic pressure, which is generated by a pressure intensifier, is converted into argon gas pressure by an

accumulator, and this converted argon gas pressure is applied via high pressure valves upon each of the 15 test pieces which are aligned in parallel.

The so applied pressure is measured by means of KS type high pressure gauges using resistance wire strain gauges, and also by Bourdon's tube. The heating device is composed of five horizontal type heaters (mobile) and an SCR type temperature regulator. The muffle of furnace, as shown by the following Fig. 4, is of a double core structure to maintain good temperature distribution, and is a multi-chamber type by dividing the inner core into four sections by partition-plates so that three test pieces can be tested simultaneously. The heaters use nichrome wire for pyrogen. The furnace's capacity is 5.5 kVA, and the environment is air.

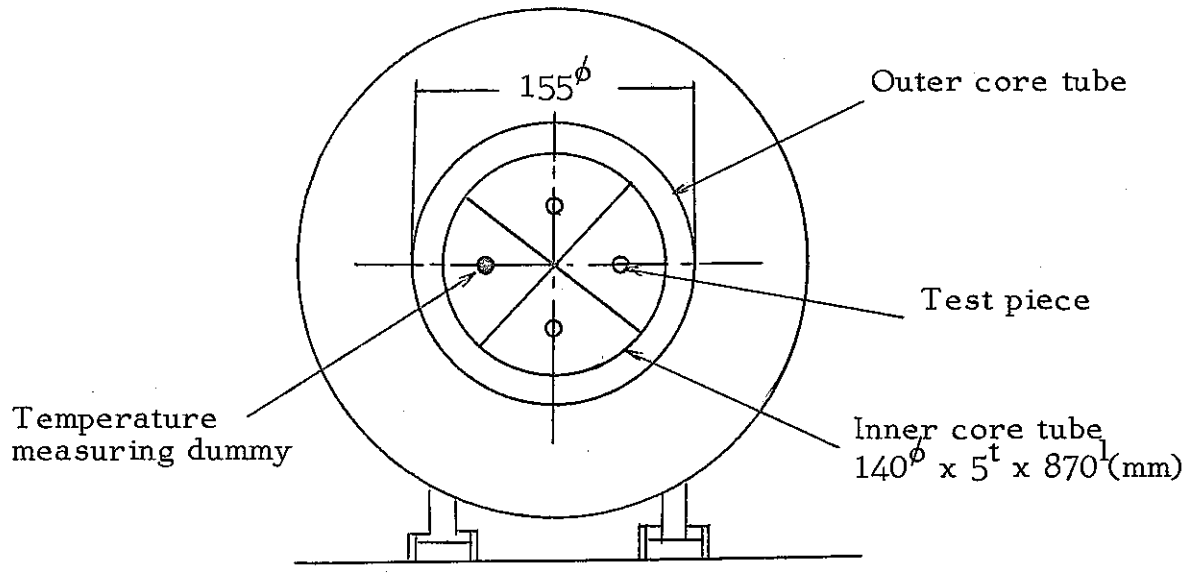

Fig. 4 Cross Section of Heating Furnace

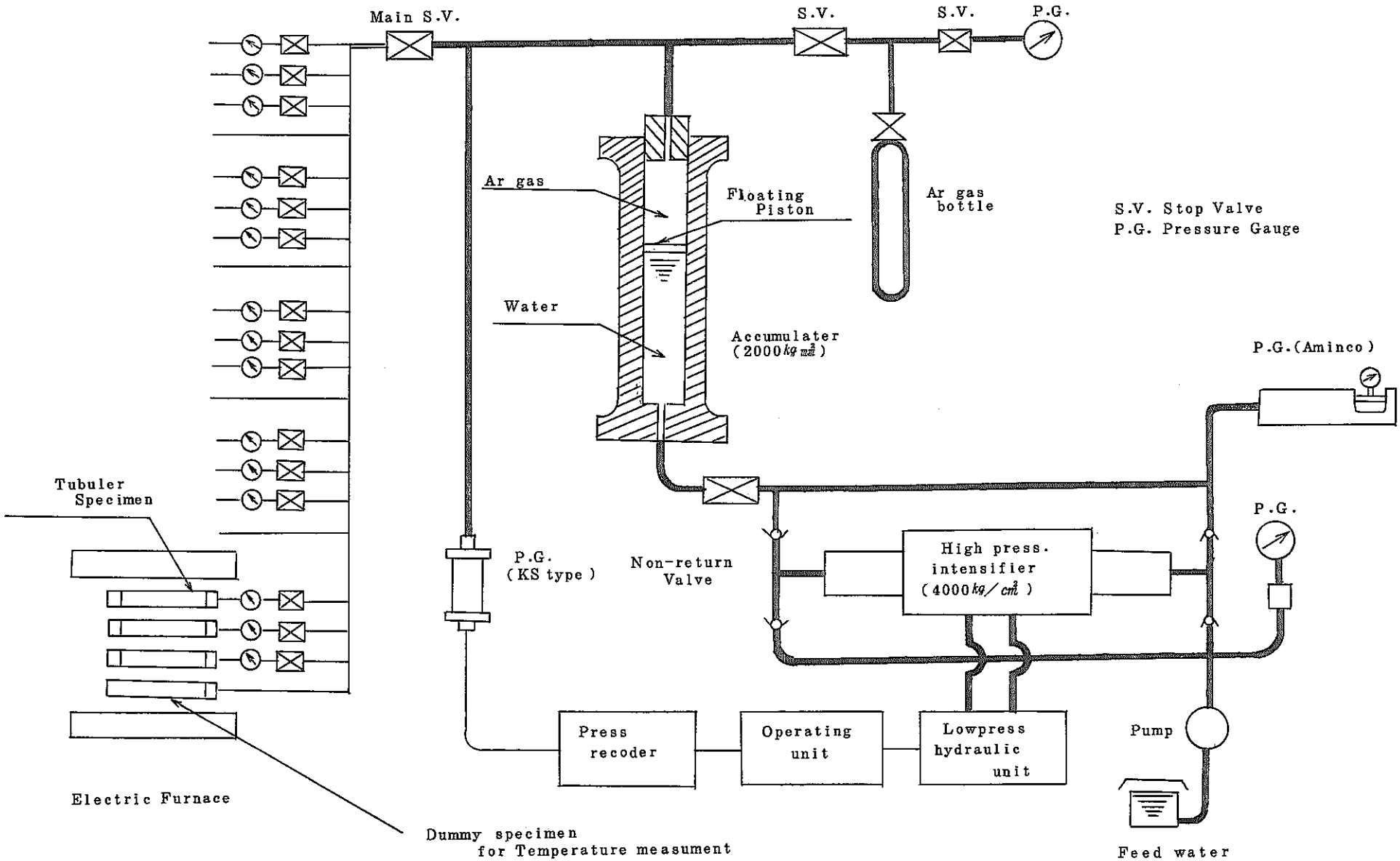
Main S.V.
S.V.
S.V.
P.G.
Ar gas
Floating Piston
Ar gas bottle
S.V. Stop Valve
P.G. Pressure Gauge
Water
Accumulater (2000kg/cm²)
P.G.(Aminco)
Tubuler Specimen
P.G. (KS type)
Non-return Valve
High press. intensifier (4000kg/cm²)
P.G.
Press recoder
Operating unit
Lowpress hydraulic unit
Pump
Electric Furnace
Dummy specimen for Temperature measument
Feed water

After having installed the test pieces inside the furnace, and packing into the test pieces the argon gas at a pressure below $\frac{1}{2}$ of the test pressure, and making sure that there is no leak of the packed gas, the pressure is lowered and temperature is raised. The temperature is measured by installing in the furnace a dummy with thermocouples at three parallel places of the test piece as shown by Fig. 4, and by use of a potentiometer. After about 8 ~ 10 hours from the temperature of the test pieces has reached the prescribed test temperature, the pressure is raised upto the prescribed level and then, the test is started.

The temperatures of the internal pressure creep rupture test and the expected rupture time are given as follows:

Test temperature	650 and 750 °C
Expected rupture time	100, 300, 1,000, and 3,000 hrs.

Repetition was made to each of the test pieces under each different test condition.

3-4 Inspection of Test Specimen after Internal Pressure Creep Rupture Tests

The appearances of specimens ruptured and internal pressure were photographed and their outside dimension were measured, and also microstructural observation by use of an optical microscope and hardness measurement were respectively conducted on all the ruptured test pieces after long-time creep rupture tests at 650 and 750 °C temperatures.

The outside diameter measurement was taken at nine points at intervals of 20mm from the tip of the total length of 200mm of each test piece, and at four points at intervals of 45 ° circumferentially

totalling thus 36 points to obtain the maximum and minimum values of the external diameter.

For the microstructural observation, samples were taken from the location about 5mm away from the actual ruptured area, and observation was performed on the structures of both longitudinal and traverse cross sections. For the sake of comparison, the test specimens were exposed to a microstructural observation before they were subjected to test.

The hardness of the cross section and the longitudinal section was measured at 9 longitudinal positions each 20mm apart using a 500 g-load Vickers' microtester.

4. Test Results

4-1 Results of High Temperature Tensile Tests

The results of the high temperature tensile test performed on the materials A and B for "MONJU" fuel cladding tube are as shown by Table 6 and Figs. 5 and 6. The values under the room temperature and at 650 °C in the diagrams are those quoted from the mill sheet. The tensile strength and 0.2 % yield strength of the materials A and B are higher with A on the lower temperature side, while no difference is observed on the higher temperature side between the two materials, nor is observed any marked difference in their elongation.

4-2 Results of Uniaxial Creep Tests

Table 7 and Figs. 7 and 8 represent the results of the uniaxial creep test on the materials A and B for "MONJU" fuel cladding tube. The minimum creep rate under the identical conditions is smaller with the material B.

4-3 Results of Internal Pressure Creep Rupture Tests

The results of the internal pressure creep rupture test performed on the materials A, B and C for "JOYO MK-II" fuel cladding tube and on the material C for "MONJU" fuel cladding tube are shown by Table 8 and Figs. 9 and 10. The results of the test on the materials for "JOYO MK-II" fuel cladding tube at 650 °C indicate a higher strength of the material B than that of A.

The similar trend is noticed at the temperature of 750 °C, and the materials B and C for "JOYO MK-II" fuel cladding tube and C for "MONJU" fuel cladding tube indicate higher strength than in the case

of the material A. But the difference seems to be narrowed under a prolonged test.

The mean values of this test and the 4th internal pressure creep rupture test are compared with the hoop stress values obtained by the expression of mean diameter. The result, as is shown by Fig. 11, show hardly any difference of strength of the material A at either 650 °C or 750 °C comparing with the result of the 4th test, while in the case of the material B and C, their strength has become higher at both temperature. Also between B and C, there is noticed hardly any difference in their strength at 750 °C.

4-4 Results of Inspection of Test Specimen after Internal Pressure Creep Rupture Tests

Photos 4-1 ~ 4-6 show the appearance of the test pieces after internal pressure creep rupture.

Figs. 13 ~ 26 represent the post-test outside diameter expansion rate (Δ D/D.) of the test pieces.

Photos 5 ~ 7 show the microstructure of the ruptured test pieces after prolonged tests at various test temperatures, and Figs. 27 ~ 29 represent their hardness distribution.

The post-rupture outside diameter expansion rate is about two times larger with A material than in the case of B material at 650 °C. At 750 °C, A material shows a larger expansion rate than in the case of B and C materials, and also of C material for "MONJU" fuel cladding tube when the test time is short. But as the test time becomes longer, the expansion rate of these latter materials, namely B, C for "JOYO MK-II" and C for "MONJU", also becomes larger.

The structure of the test pieces which ruptured after prolonged

tests at various test temperatures shows in the case of both materials A and B certain precipitation of σ-phase in the grain boundary at 650 °C. Although any direct comparison is difficult because of difference of actual test conditions, it is considered A-material has more σ-phase precipitation than in the case of B-material.

At 750 °C, these test pieces indicate a great amount of σ-phase precipitation, and from the state of their structure and the hardness decline as shown by Figs. 28 and 29, it is considered that a considerable amount of recrystallization has progressed.

4-5 Discussion on the difference in creep properties of A and B materials

Fig. 12 shows the effect of grain size on the creep rupture strength of 20% cold worked 18-8 Mo austenitic stainless steels containing 3 ppm and 17 ppm boron. As is evident from the diagram, as becoming finer the grain size, the creep rupture strength declines. But such strength decline becomes more evident as lower is boron. Both A-material and B-material have about 3 ppm of boron, while their grain size is ASTM No. 9.5 for A-material and ASTM No. 7 for B-material. This corresponds with respectively the solid circle and hollow circle in the diagram, and shows a trend of quite a good agreement with the results shown in Fig. 11. From this fact, the difference in creep strength of A and B materials is considered because of the difference in their respective grain size, and also from Fig. 12, it is considerable that the strength decline which is caused by the finer grain size can be improved by raising the content of boron.

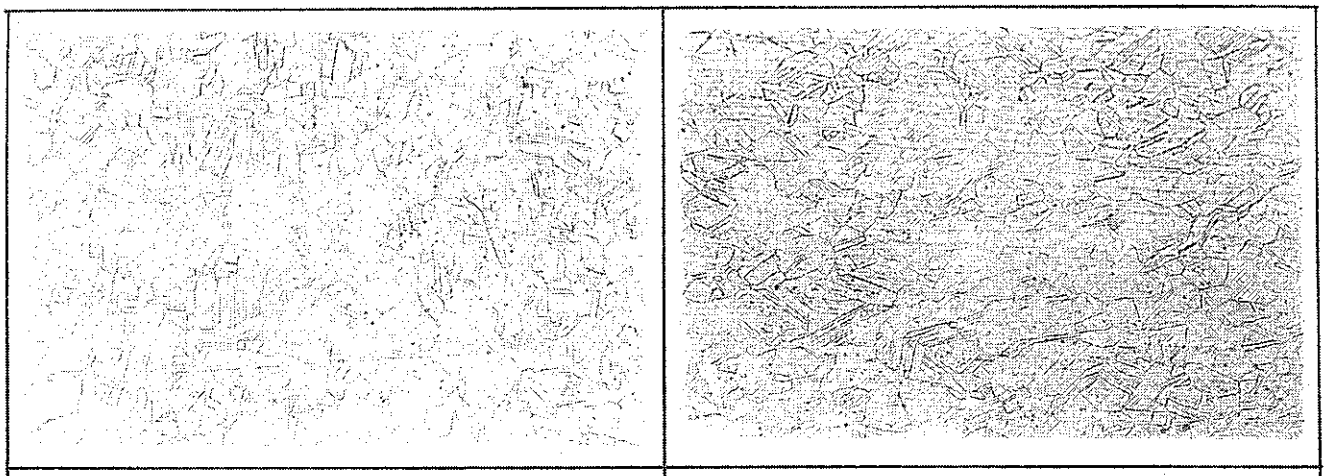

Traverse cross section	Longitudinal cross section
Material A for "JOYO MK-II"	

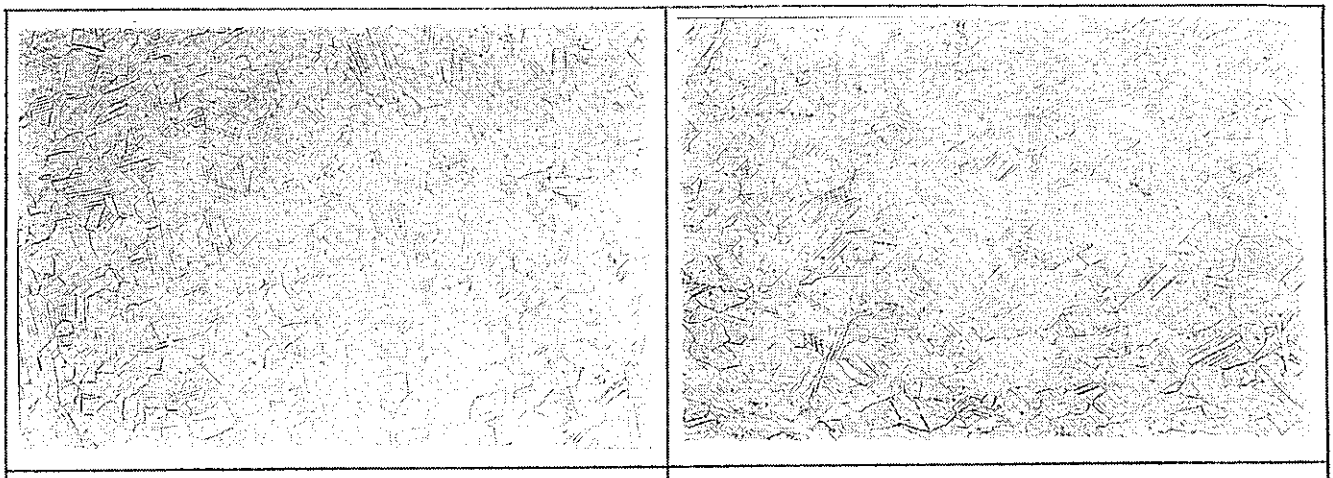

Traverse cross section	Longitudinal cross section
Material A for "MONJU"	

Photo-1. Microstructure of Test Specimen (x400)

Item \ Material		"JOYO MK-II" Core A (K0708-10)	"MONJU" Core A (K3105-13)
Hv 500gr	Traverse Cross Section	282	283
	Longitudinal Cross Section	285	269
Grain Size (ASTM No.)		9.5	9.5

Table 3. Hardness and Grain Size of Test Specimen

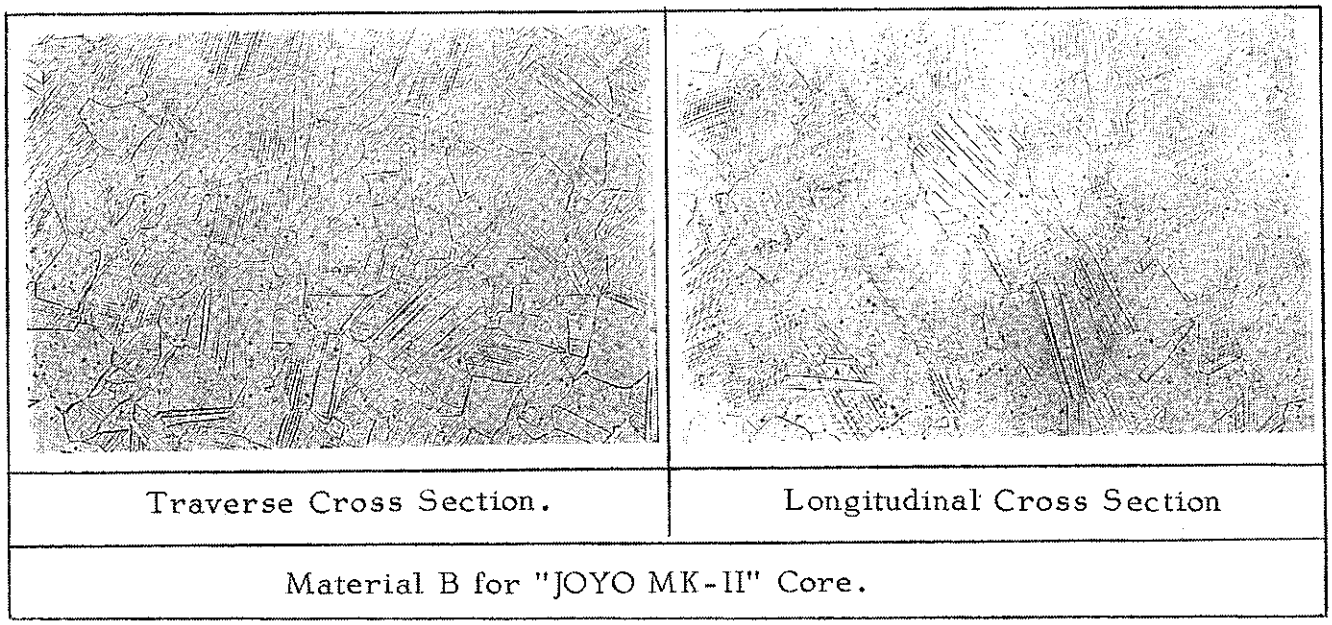

Traverse Cross Section.	Longitudinal Cross Section

Material B for "JOYO MK-II" Core.

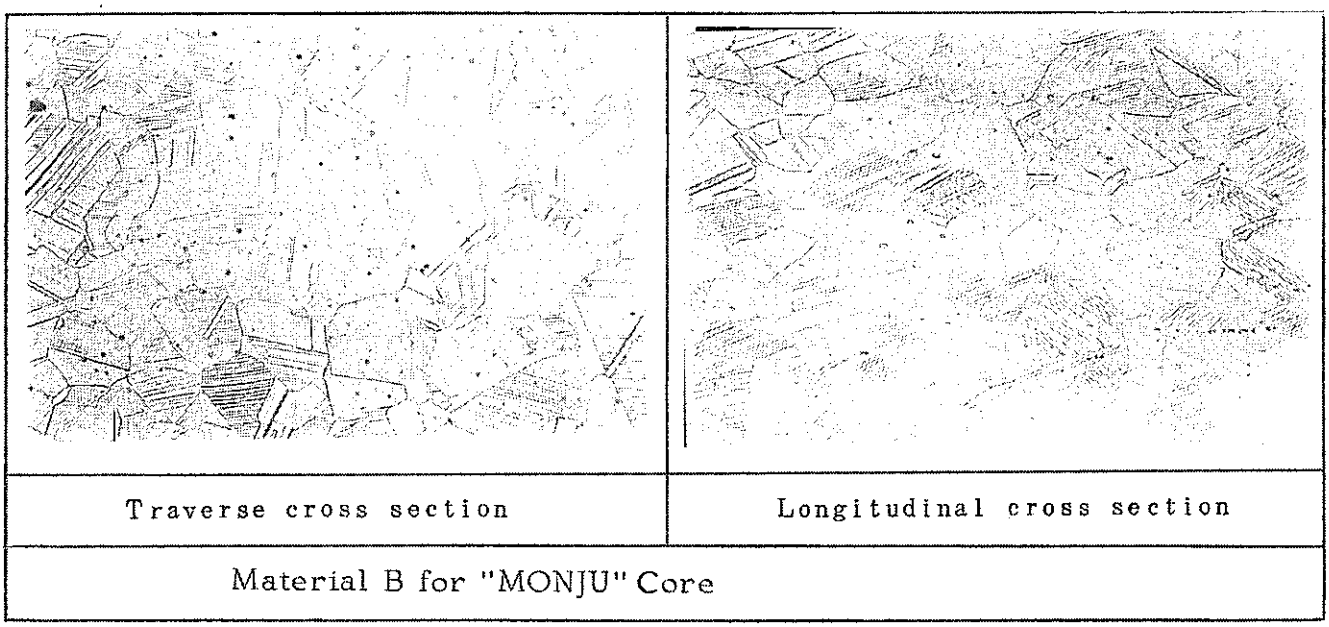

Traverse cross section	Longitudinal cross section

Material B for "MONJU" Core

Photo-2. Microstructure of Test Specimen (x400)

Item \ Material		"JOYO MK-II" Core B (S0730-10)	"MONJU" Core B (S3250-13)
Hv 500gr	Traverse Cross Section	281	273
	Longitudinal Cross Section	270	281
Grain Size (ASTM No.)		7.0	7.0

Table 4. Hardness & Grain Size of Test Specimen

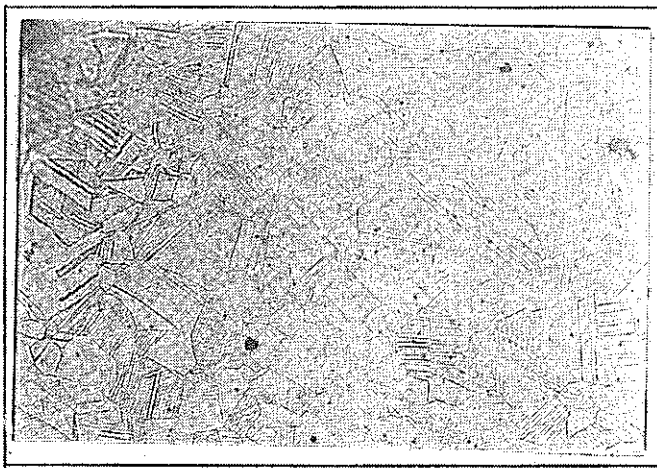

Traverse Cross Section.

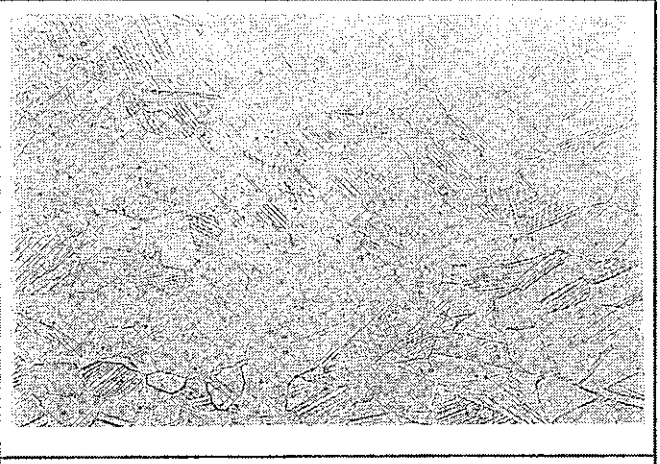

Longitudinal Cross Section.

Material C for "JOYO MK-II" Core.

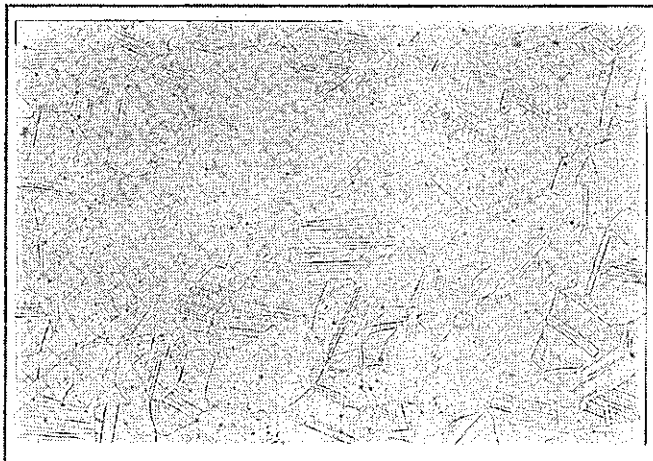

Traverse cross section

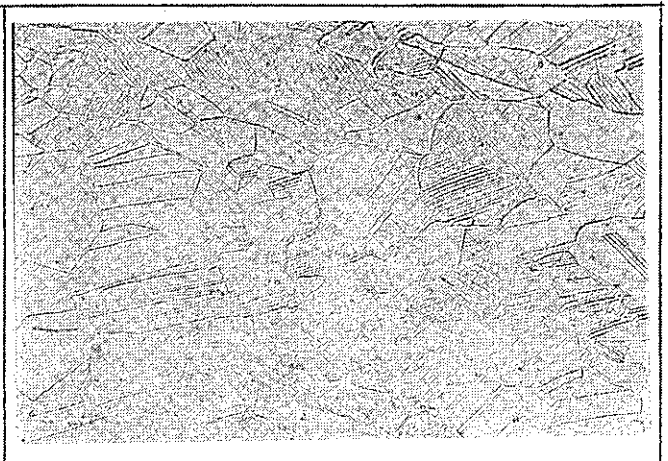

Longitudinal cross section

Material C for "MONJU" Core.

Photo-3. Microstructure of Test Specimen (x400)

Item \ Material		"JOYO MK-II" Core C (S0026-9)	"MONJU" Core C (S3018-17)
Hv 500gr	Traverse Cross Section	287	281
	Longitudinal Cross Section	292	287
Grain Size (ASTM No.)		7.0	7.0

Table 5. Hardness and Grain Size of Test Specimen

Temp. (°C)	No. of Test Specimen	Tensile Strength (Kg/mm^2)	0.2% Yield Strength (Kg/mm^2)	Elongation (%)
400	K3119-1	67.9	60.3	6.2
500	K3111-1	64.5	56.8	5.2
600	K3120-1	56.8	50.3	6.2
700	K3106-1	42.5	32.5	21.2
750	K3124-1	35.1	26.8	27.0
800	K3101-1	27.0	17.6	31.2
400	S3250-1	64.4	56.8	4.1
500	S3239-1	61.8	55.7	6.2
600	S3258-1	55.6	50.3	8.2
700	S3240-1	42.3	33.0	17.5
750	S3205-1	33.5	24.5	25.0
800	S3254-1	27.8	20.5	26.0

Table 6. Results of High Temperature Tensile Tests

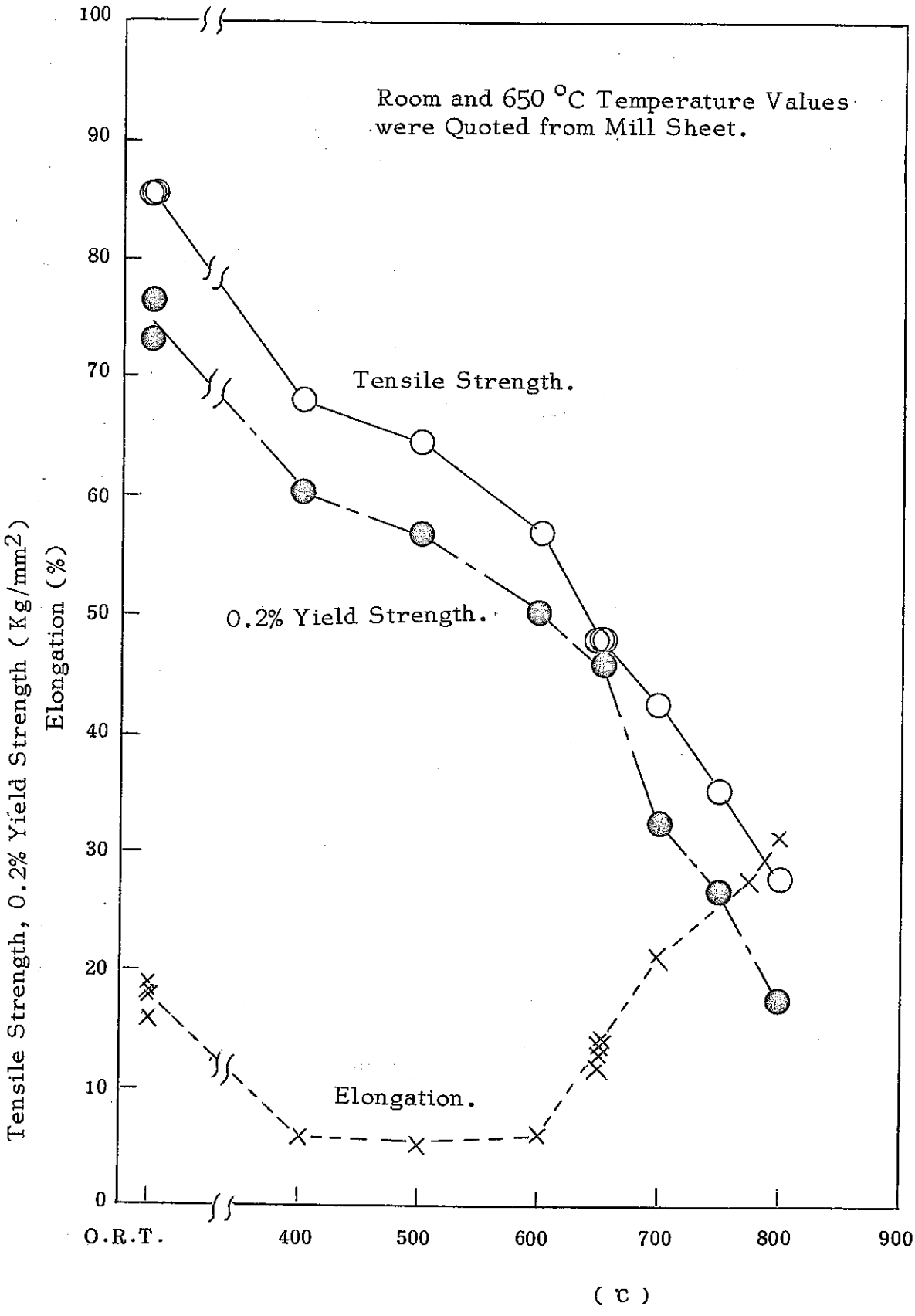

Fig. 5. High Temperature Tensile Tests (A Material)

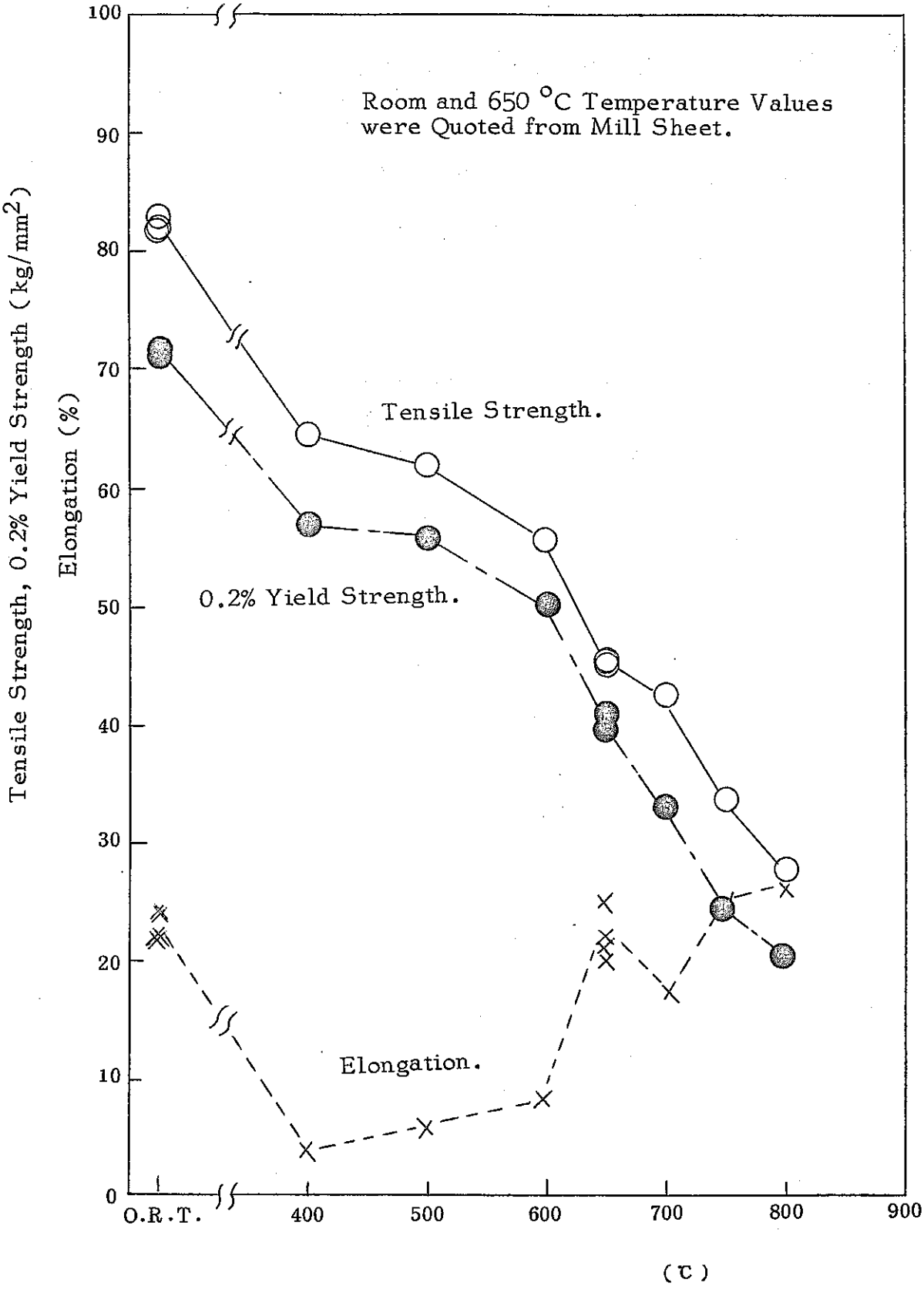

Fig. 6. High Temperature Tensile Tests (B Material)

Kind of Material	No. of Test Specimen	Temp. (°C)	Stress (Kg/mm^2)	Min. Creep Rate (%/hr)	Test Time (hr)
"MONJU" A	K3106-12	700	12.0	9.3×10^{-3}	226.5 Rptrd
	K3104-12	700	7.0	1.1×10^{-3}	860.0 Rptrd
	K3105-12	700	4.0	3.6×10^{-4}	3562.0 Stop
	K3111-12	700	2.0	1.0×10^{-4}	2635.0 Stop
"MONJU" B	S3250-12	700	12.0	1.6×10^{-3}	835.5 Rptrd
	S3240-12	700	7.0	4.8×10^{-4}	2668.0 Stop
	S3242-12	700	4.0	1.4×10^{-4}	3211.0 Stop
	S3239-12	700	2.0	1.0×10^{-4}	2959.0 Stop

Table 7. Results of Uniaxial Creep Test.

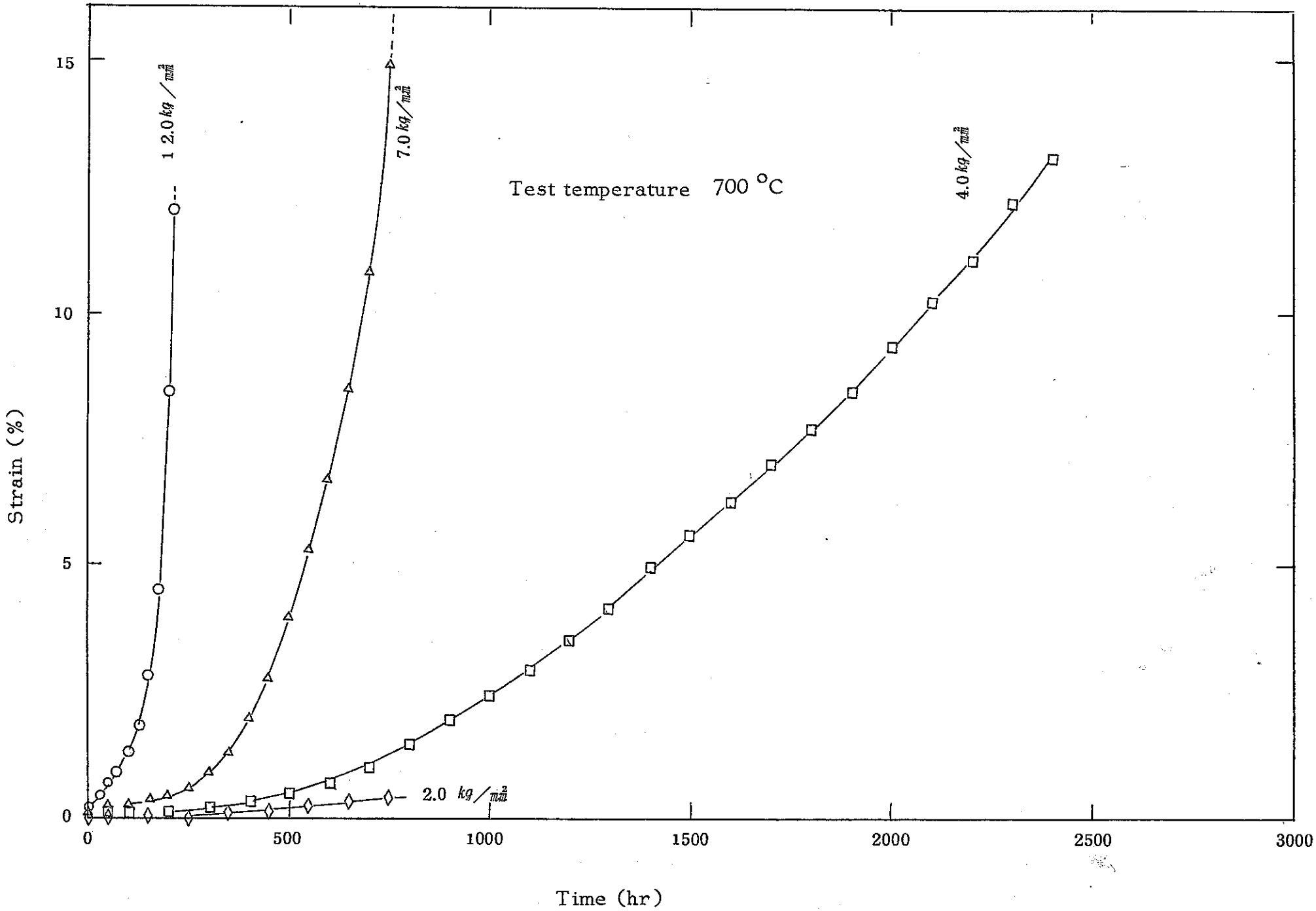

Fig. 7. Creep Curves of Materials A and B for "MONJU" Fuel Cladding Tube at 700 °C.

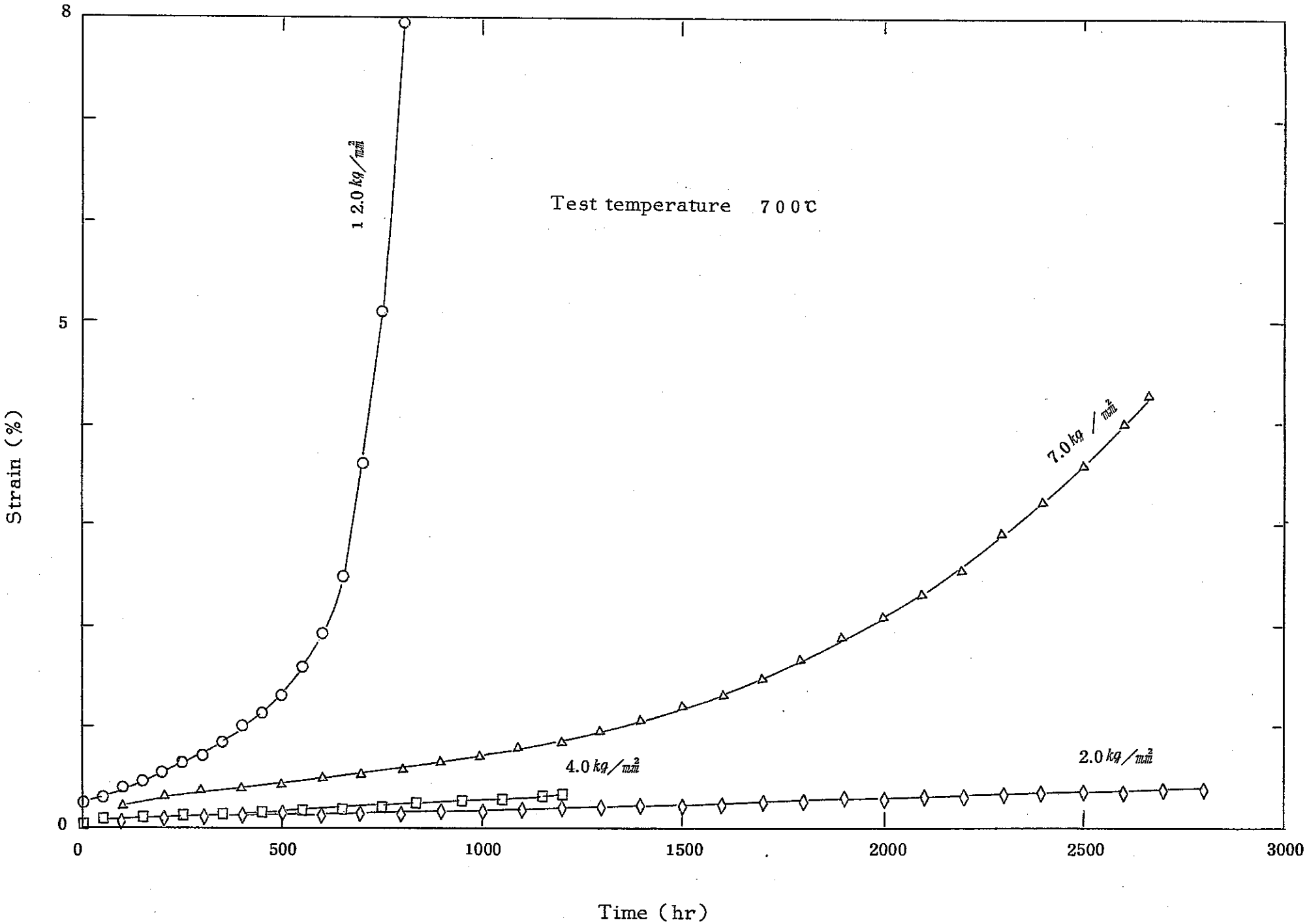

Fig. 8. Creep Curves of Materials A and B for "MONJU" Fuel Cladding Tube at 700 °C.

Material	No. of Test Specimen	Temp. (°C)	Pressure (Kg/mm^2)	Time to Rupture (hr)
"JOYO MK-II" Core A	K0205-4	650	380	121
	K0121-4	"	330	151
	K0208-3	"	260	470
	K0205-3	"	210	803
	K0129-3	"	165	2126
"JOYO MK-II" Core B	S0736-2	650	380	105
	S0701-4	"	330	220
	S0736-3	"	260	1540
	S0742-2	"	200	4012
"JOYO MK-II" Core A	K0208-2	750	160	55
	K0121-2	"	130	97
	K0205-1	"	90	210
	K0227-1	"	60	501
	K0197-4	"	45	2120
"JOYO MK-II" Core B	S0742-1	750	160	150
	S0730-2	"	130	264
	S0664-4	"	100	1002
	S0742-3	"	70	1840
"JOYO MK-II" Core C	S0129-1	750	200	40
	S0146-1	"	160	190
	S0107-2	"	100	898
	S0117-1	"	70	1630
"MONJU" Core C	S3019-1	750	200	60
	S3014-3	"	160	304
	S3019-4	"	100	1066
	S3014-2	"	70	1720

Table 8. Results of Internal Pressure Creep Rupture Tests

Fig. 9. Results of 5th Internal Pressure Creep Rupture Test

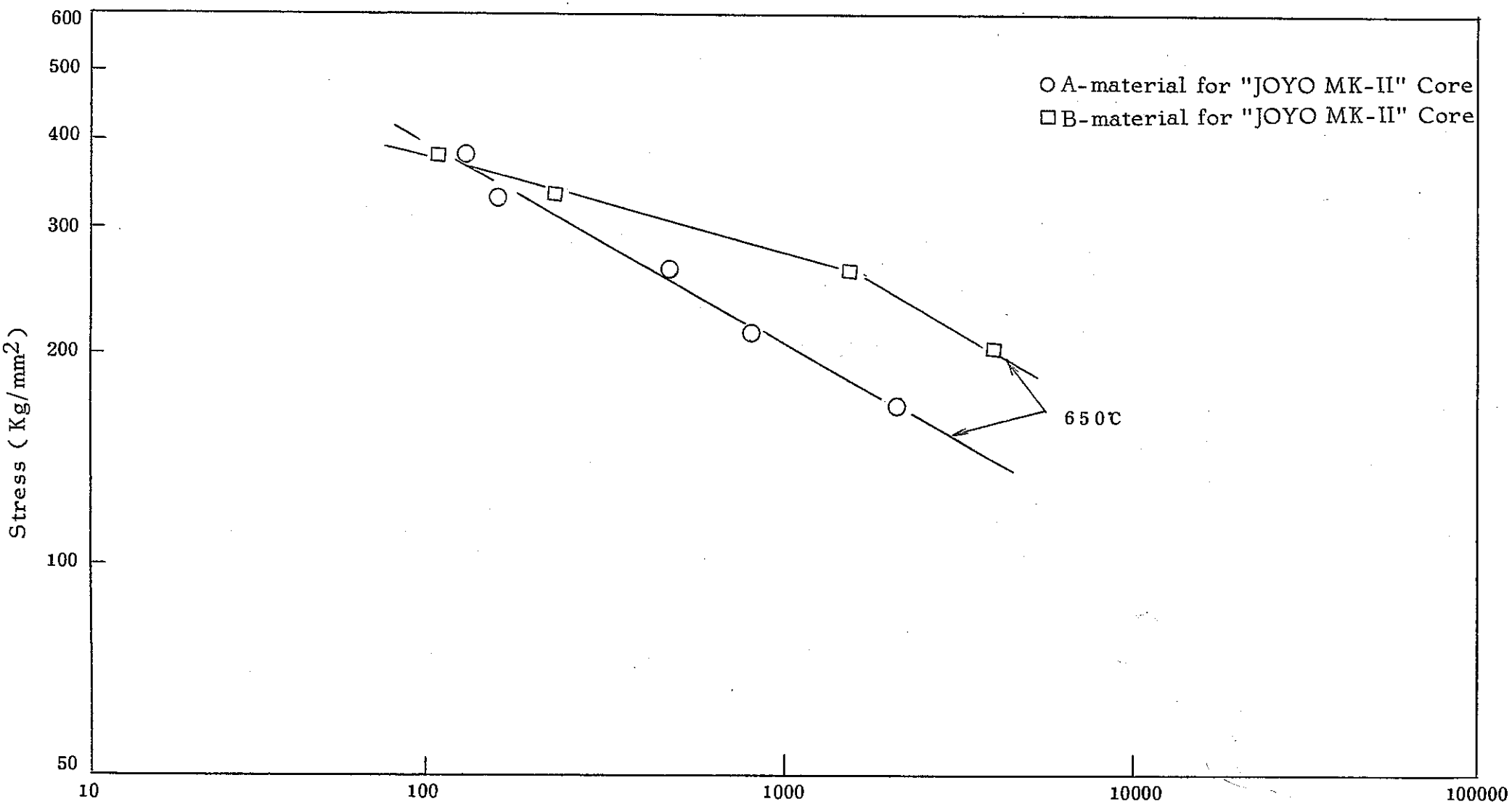

Fig. 10. Results of 5th Internal Pressure Creep Rupture Test (750℃)

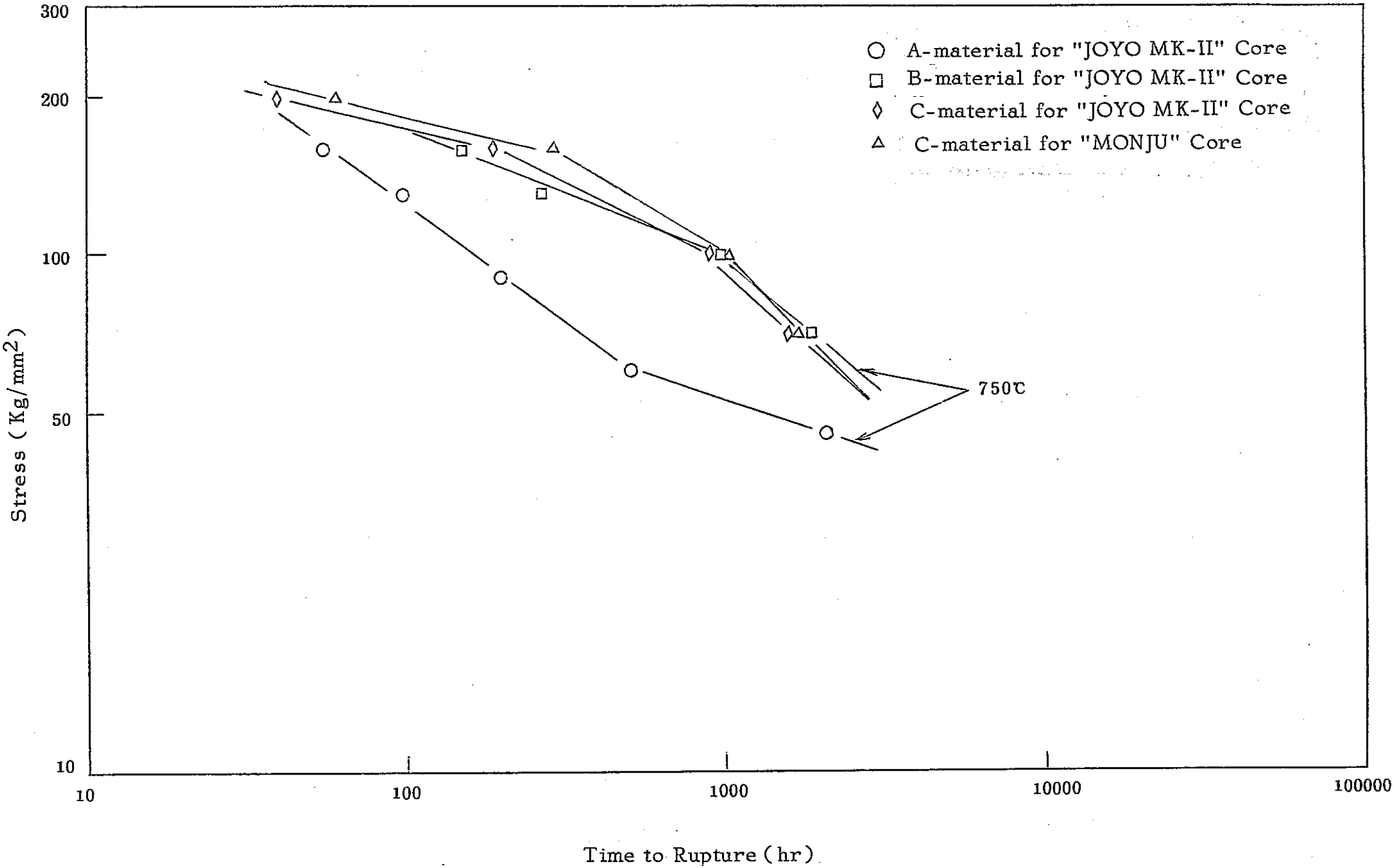

Fig. 12. Effect of Grain Size upon Creep Rupture Strength
(by plate shaped test specimens)

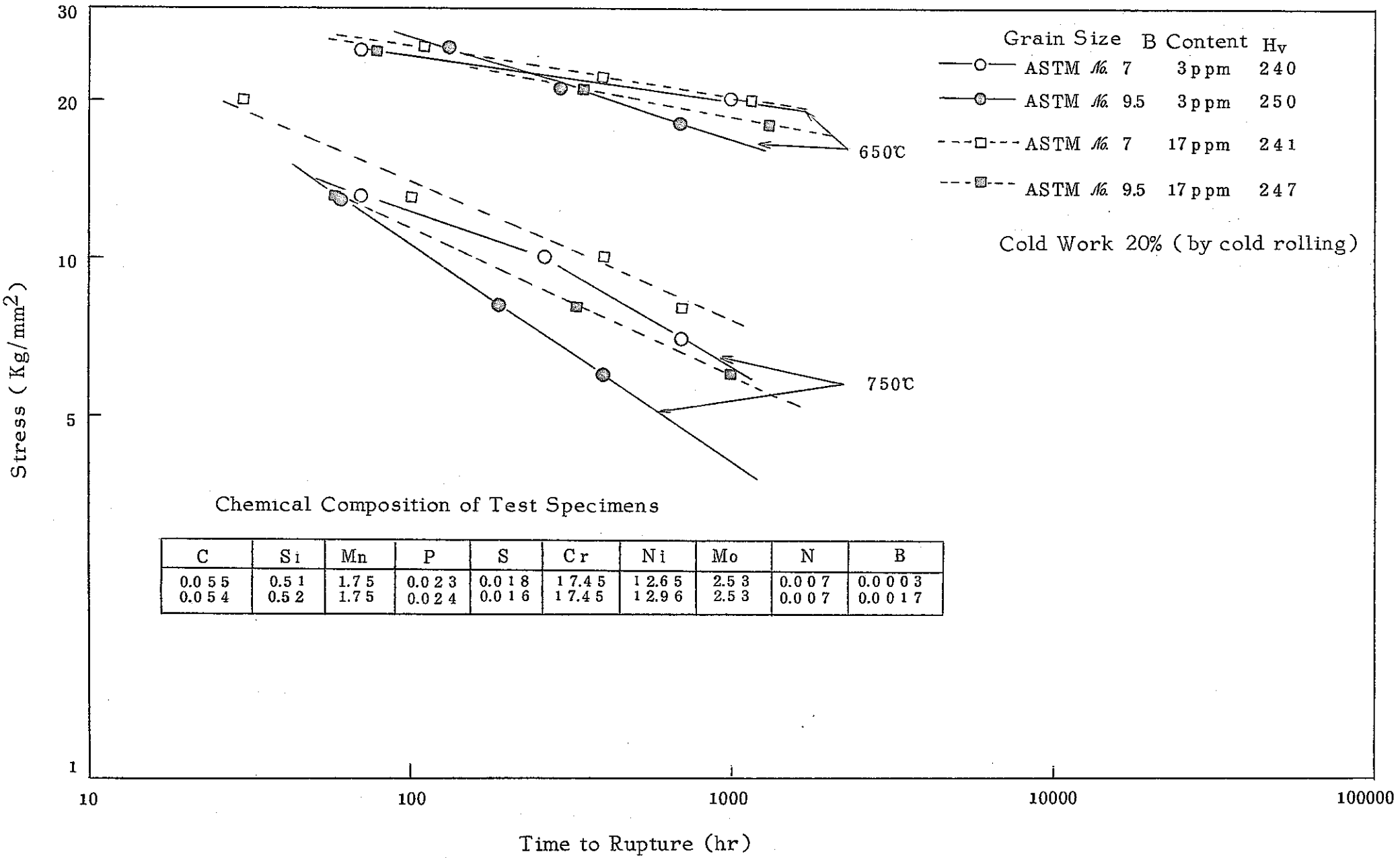

Chemical Composition of Test Specimens

C	Si	Mn	P	S	Cr	Ni	Mo	N	B
0.055	0.51	1.75	0.023	0.018	17.45	12.65	2.53	0.007	0.0003
0.054	0.52	1.75	0.024	0.016	17.45	12.96	2.53	0.007	0.0017

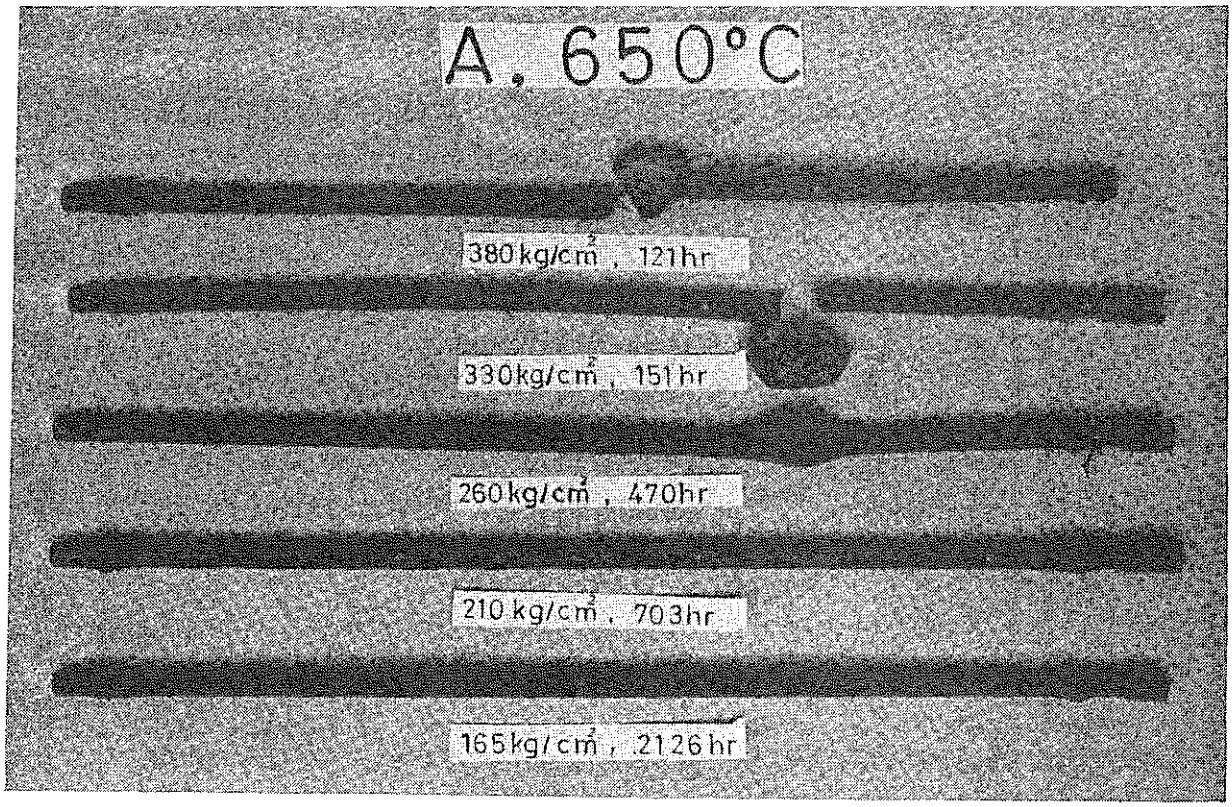

Photo 4-1. Appearance of Test Pieces after Internal Pressure Creep Rupture Tests (A material)

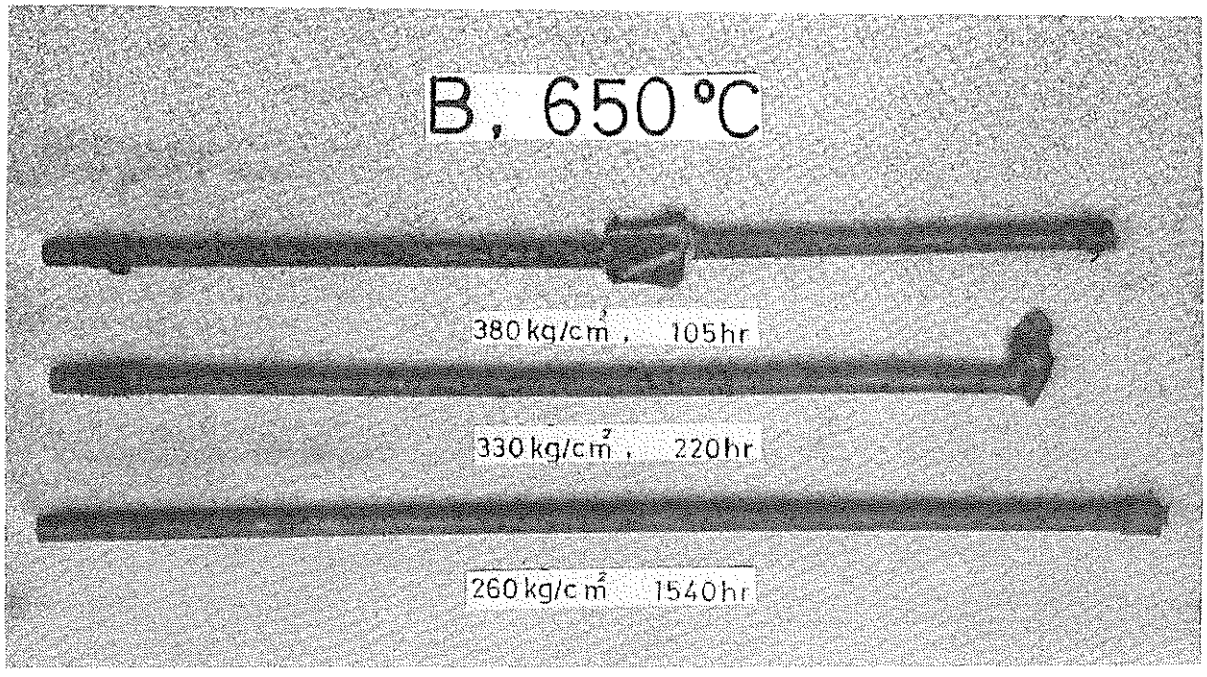

Photo 4-2. Appearance of Test Pieces after Internal Pressure Creep Rupture Tests (B material)

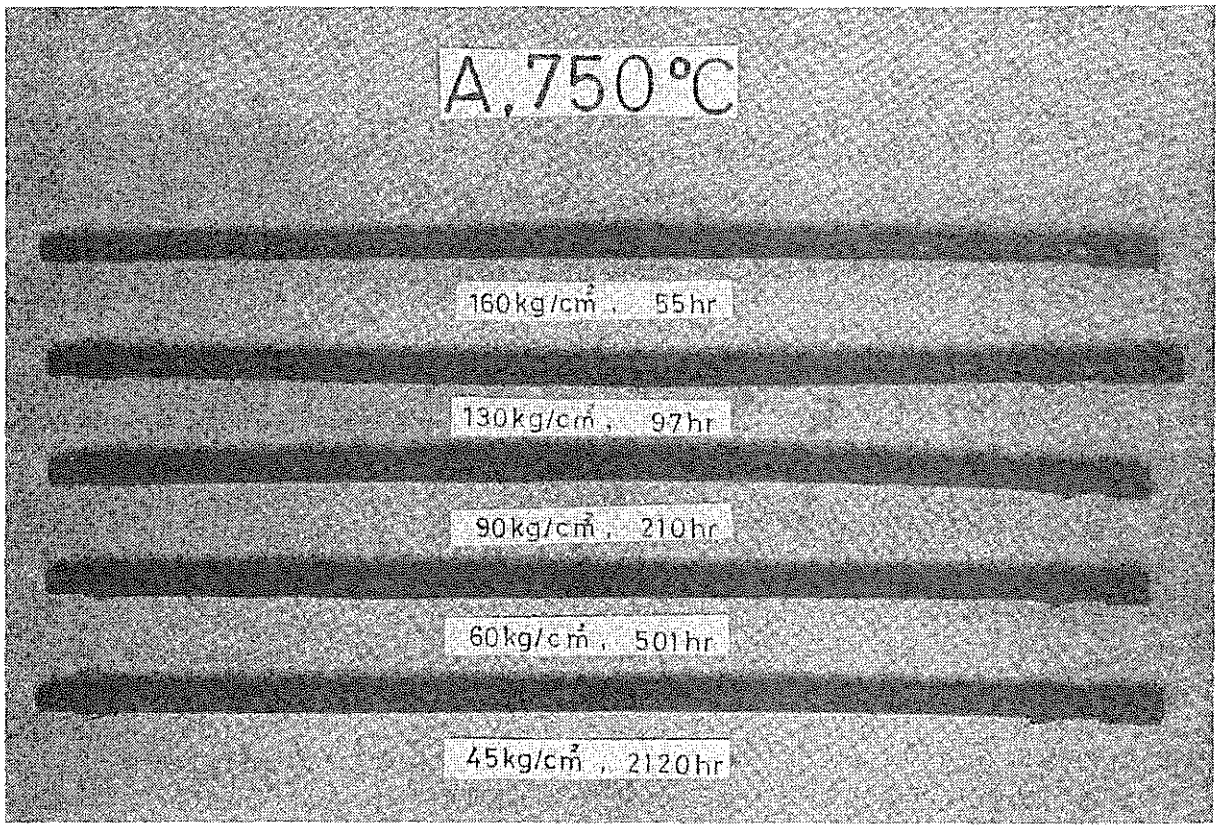

Photo 4-3. Appearance of Test Pieces after Internal Pressure Creep Rupture Tests (A material)

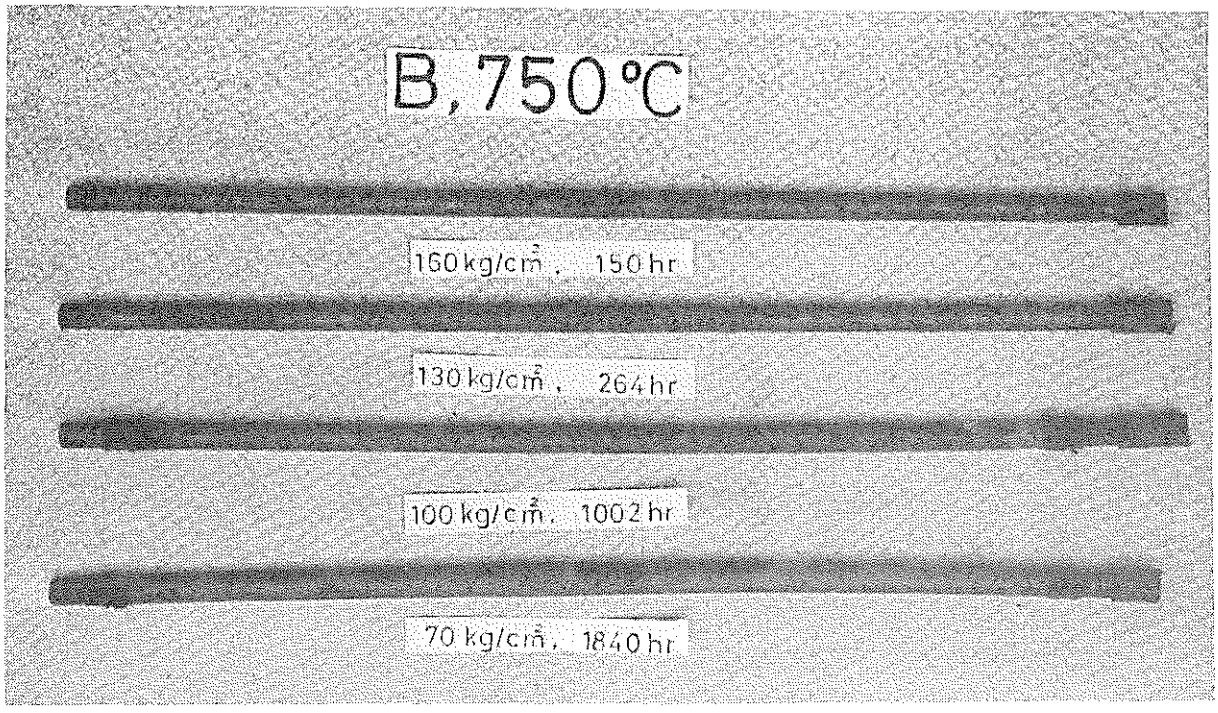

Photo 4-4. Appearance of Test Pieces after Internal Pressure Creep Rupture Tests (B material)

Fig. 11. Relation between Hoop Stress and Rupture Time Obtained by Expression of Mean Diameter.

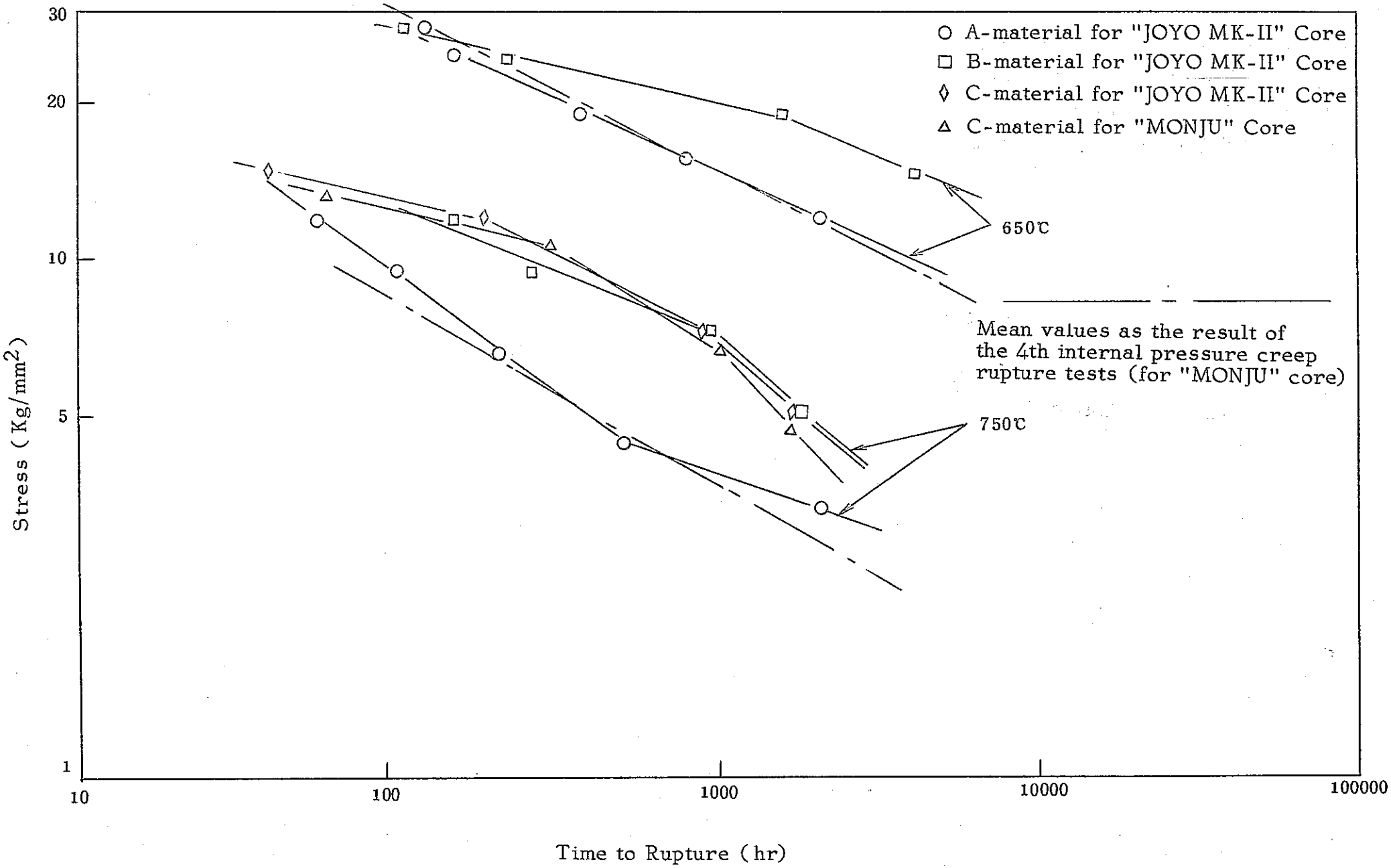

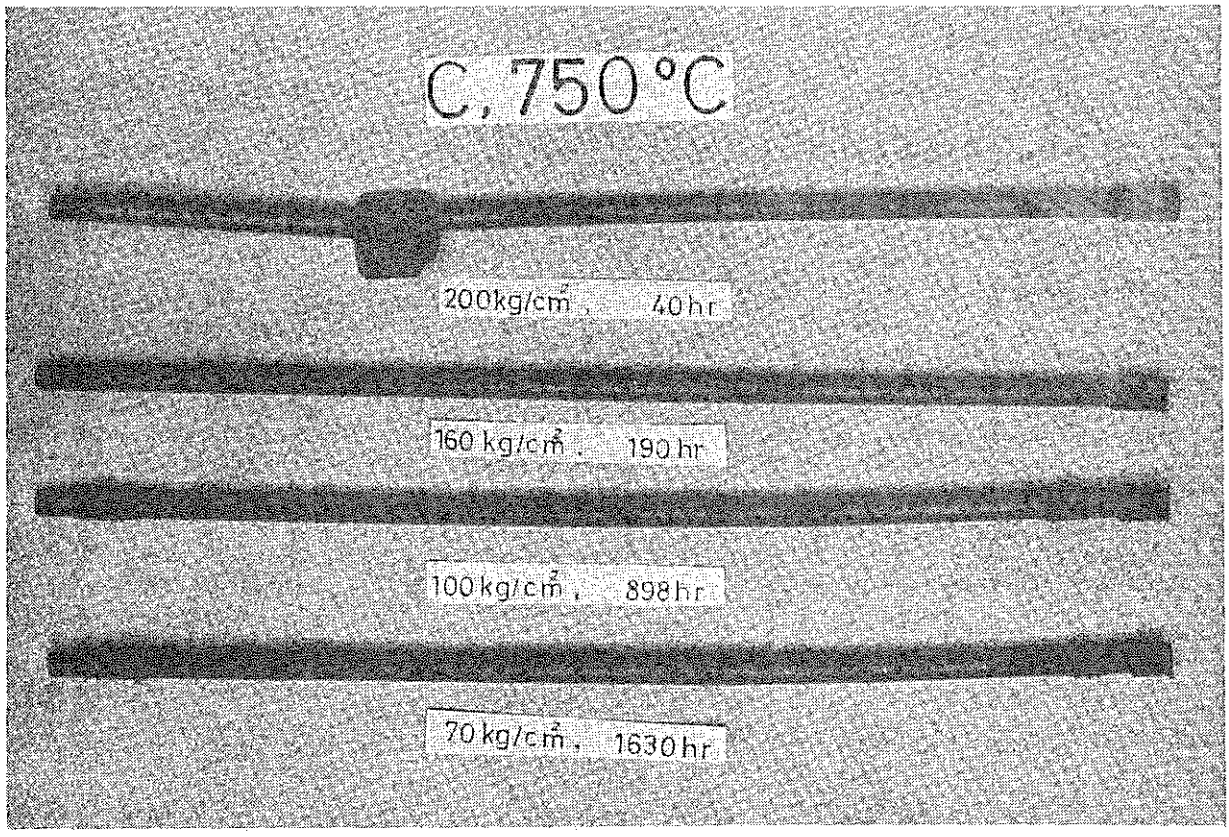

Photo 4-5. Appearance of Test Pieces after Internal Pressure Creep Rupture Tests (C material)

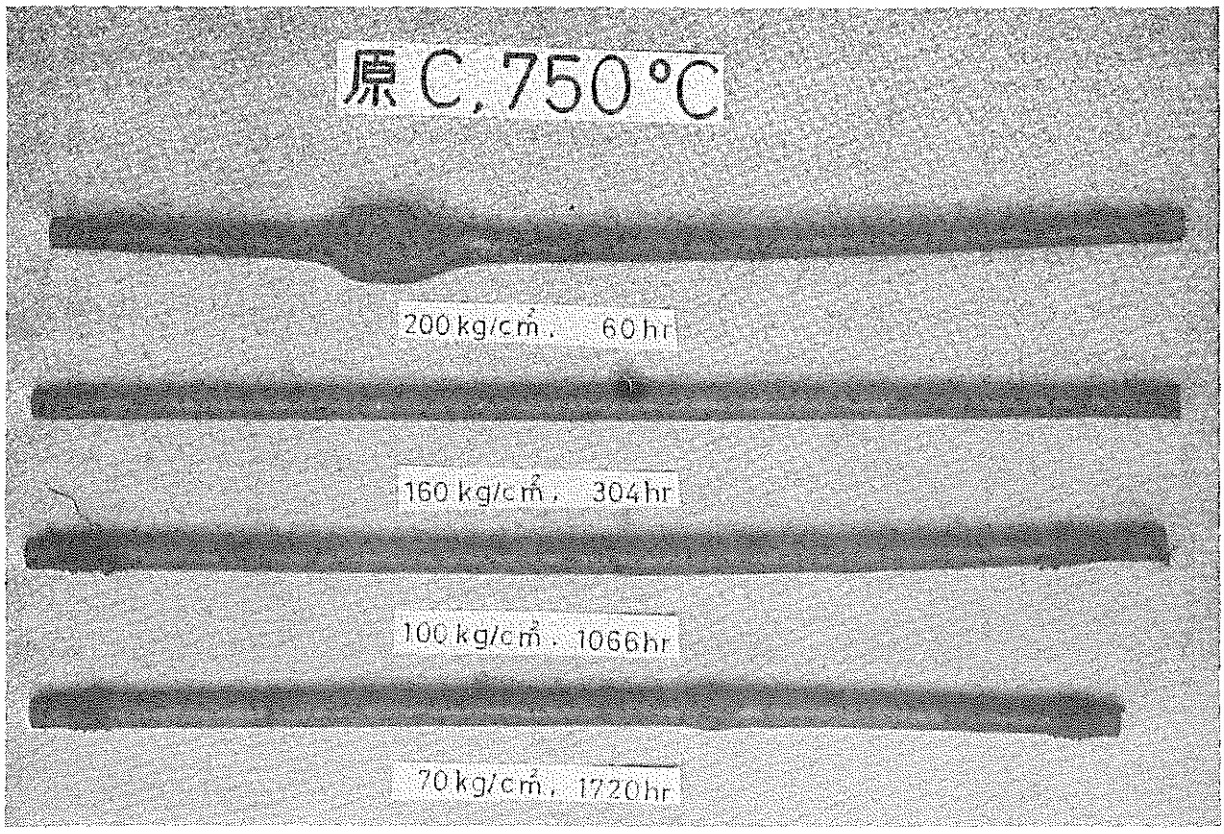

Photo 4-6. Appearance of Test Pieces after Internal Pressure Creep Rupture Tests (C material)

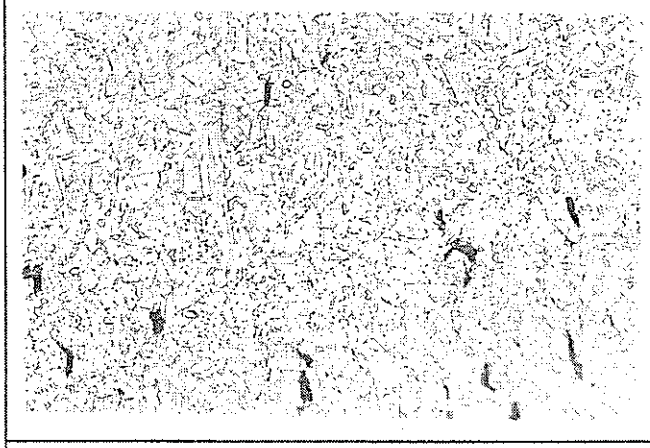

Traverse Cross Section

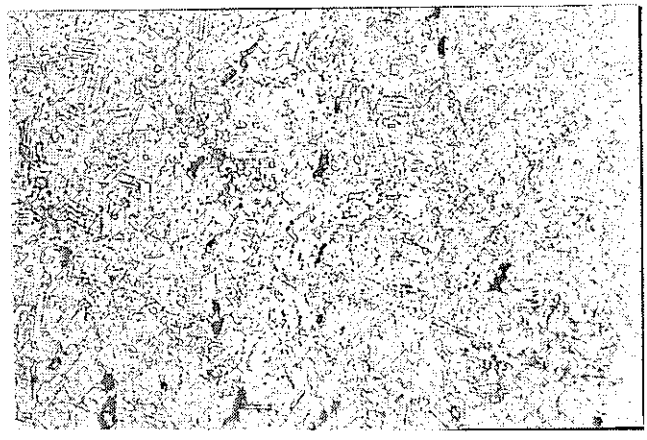

Longitudinal Cross Section

A-Material for "JOYO MK-II" Core K0129-3, 165 kg/cm^2 Ruptured at 2126 hrs.

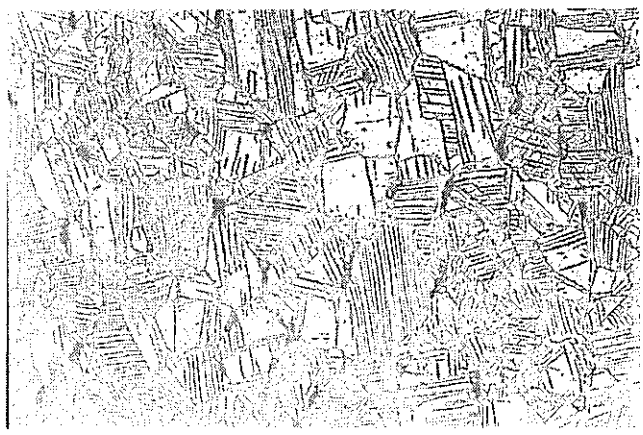

Traverse Cross Section

Longitudinal Cross Section

B-Material for "JOYO MK-II" Core S0736-3, 260 kg/cm^2 Ruptured at 1540 hrs.

Photo-5. Microstructure of Test Pieces after Long-time Rupture Test at 650 °C (x400)

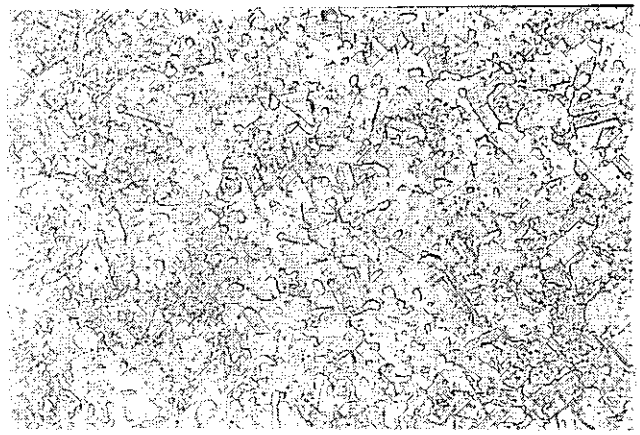

Traverse Cross Section	Longitudinal Cross Section

A-Material for "JOYO MK-II" Core K0197-4, 45 kg/cm^2 Ruptured at 2120 hrs.

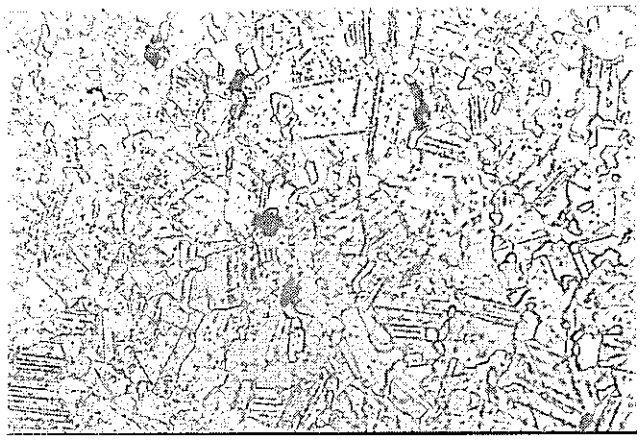

Traverse Cross Section	Longitudinal Cross Section

B-Material for "JOYO MK-II" Core S0742-3, 70 kg/cm^2 Ruptured at 1840 hrs.

Photo-6. Microstructure of Test Pieces after Long-time Rupture Test at 750 °C (x400)

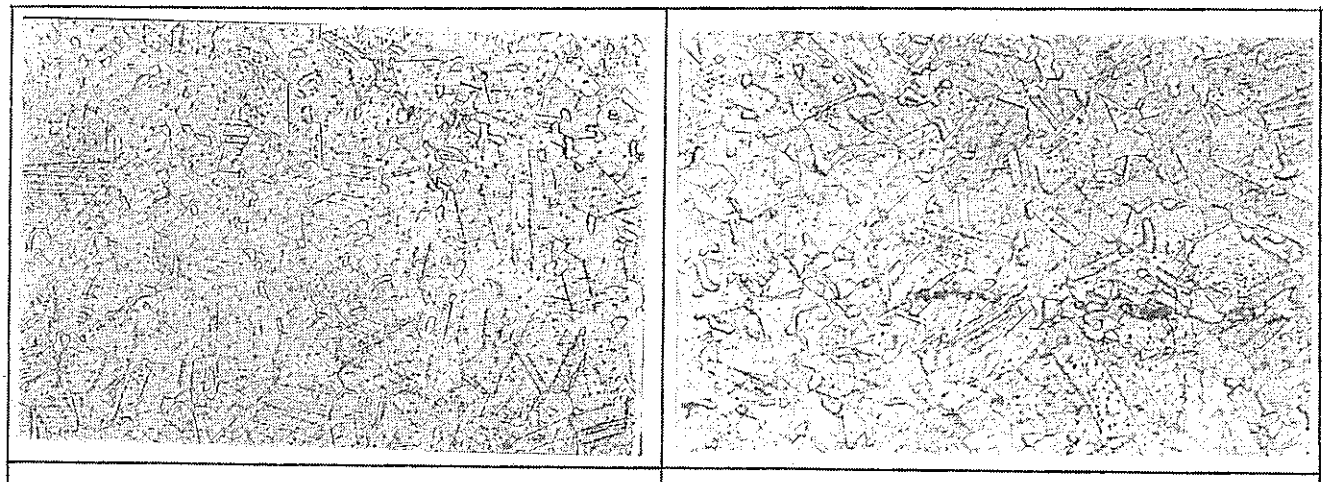

Traverse Cross Section	Longitudinal Cross Section

C-Material for "JOYO MK-II" Core S0117-1, 70 kg/cm^2 Ruptured at 1630 hrs.

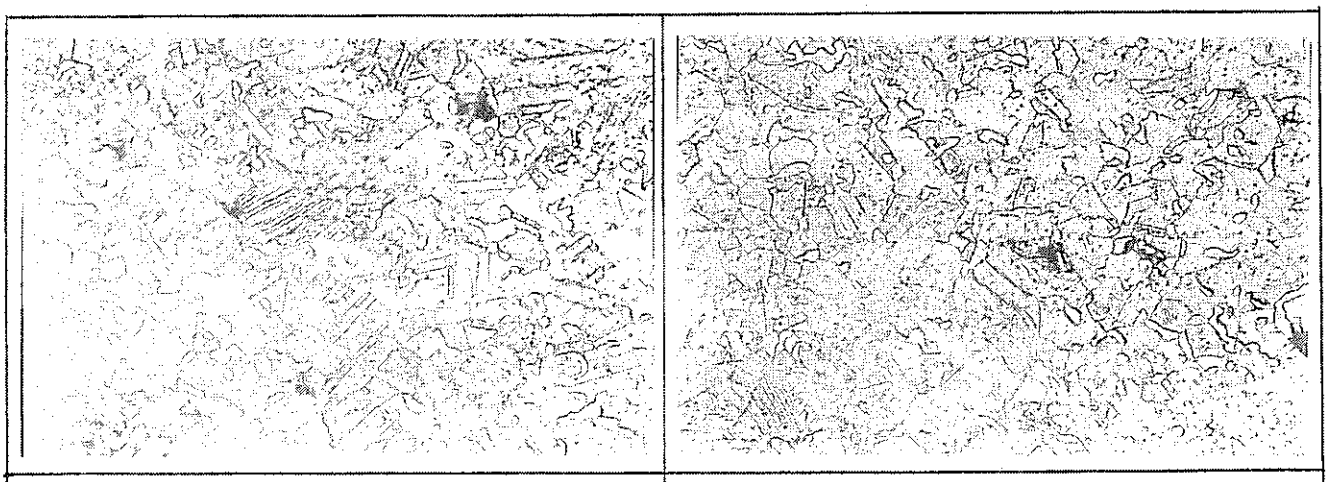

Traverse Cross Section	Longitudinal Cross Section

C-Material for "MONJU" Core S3014-2, 70 kg/cm^2 Ruptured at 1720 hrs.

Photo-7. Microstructure of Test Pieces after Long-time Rupture Test at 750 °C (x400)

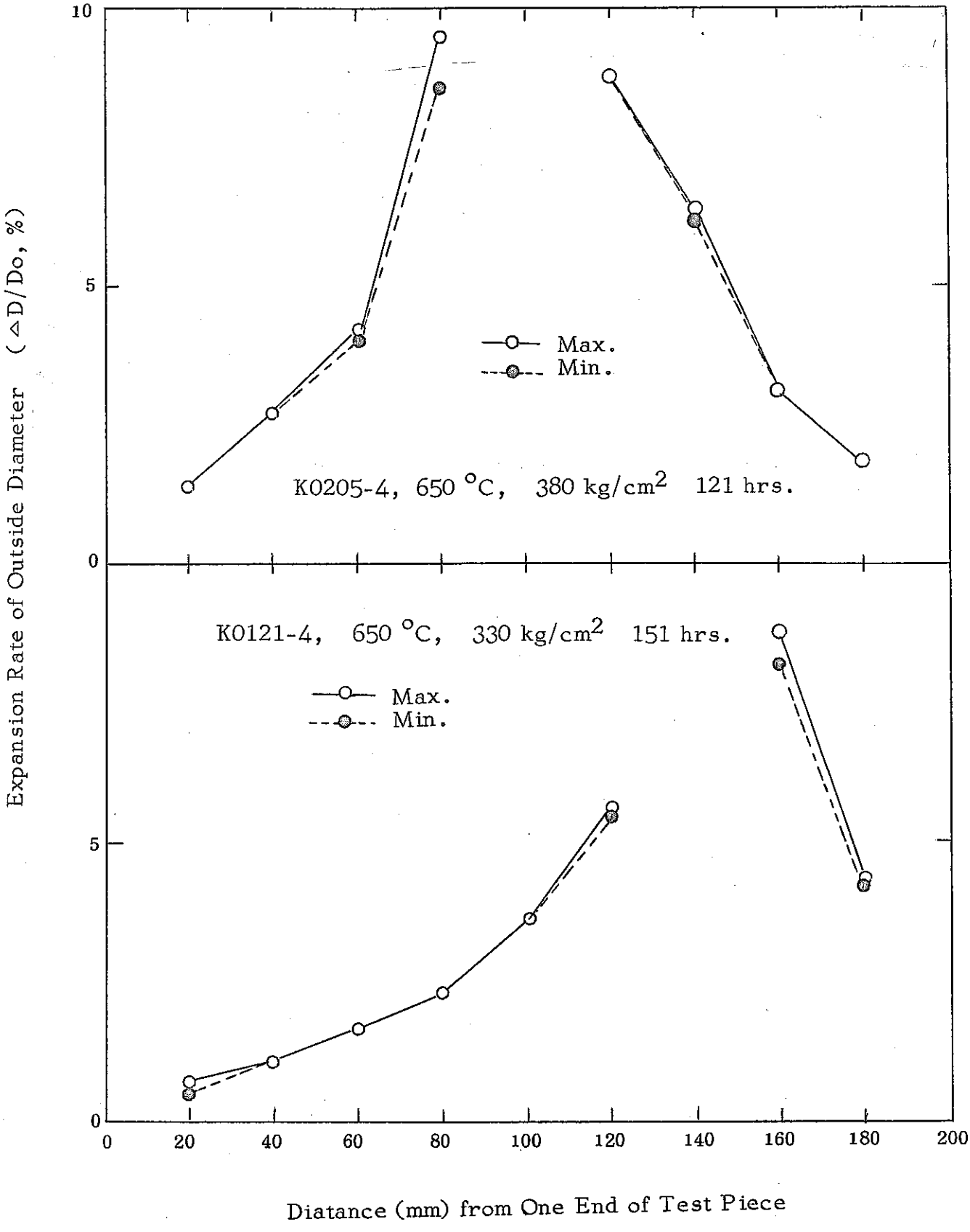

Fig. 13. Expansion Rate of Outside Diameter of Test Pieces after Rupture

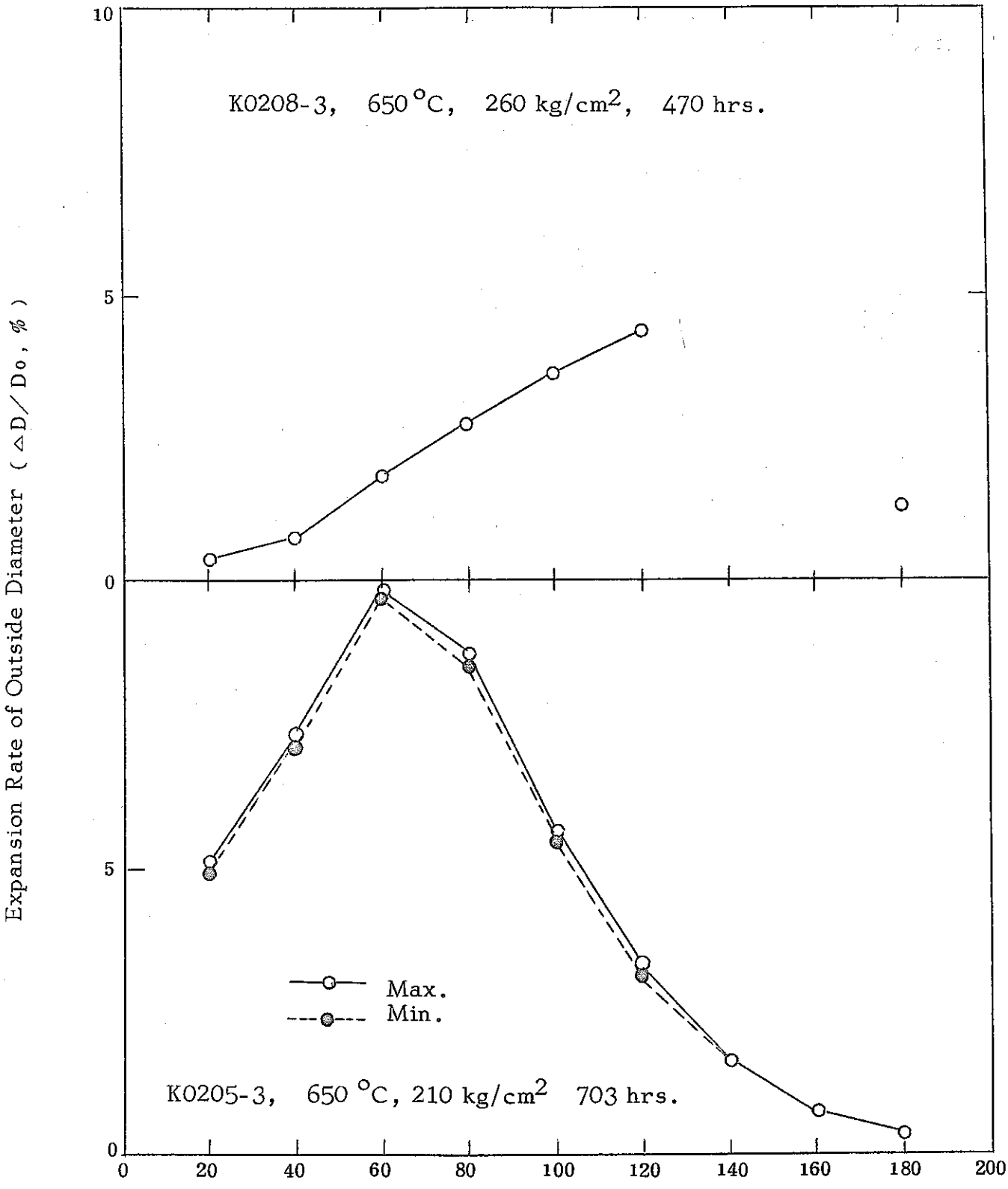

Fig. 14. Expansion Rate of Outside Diameter of Test Pieces after Rupture

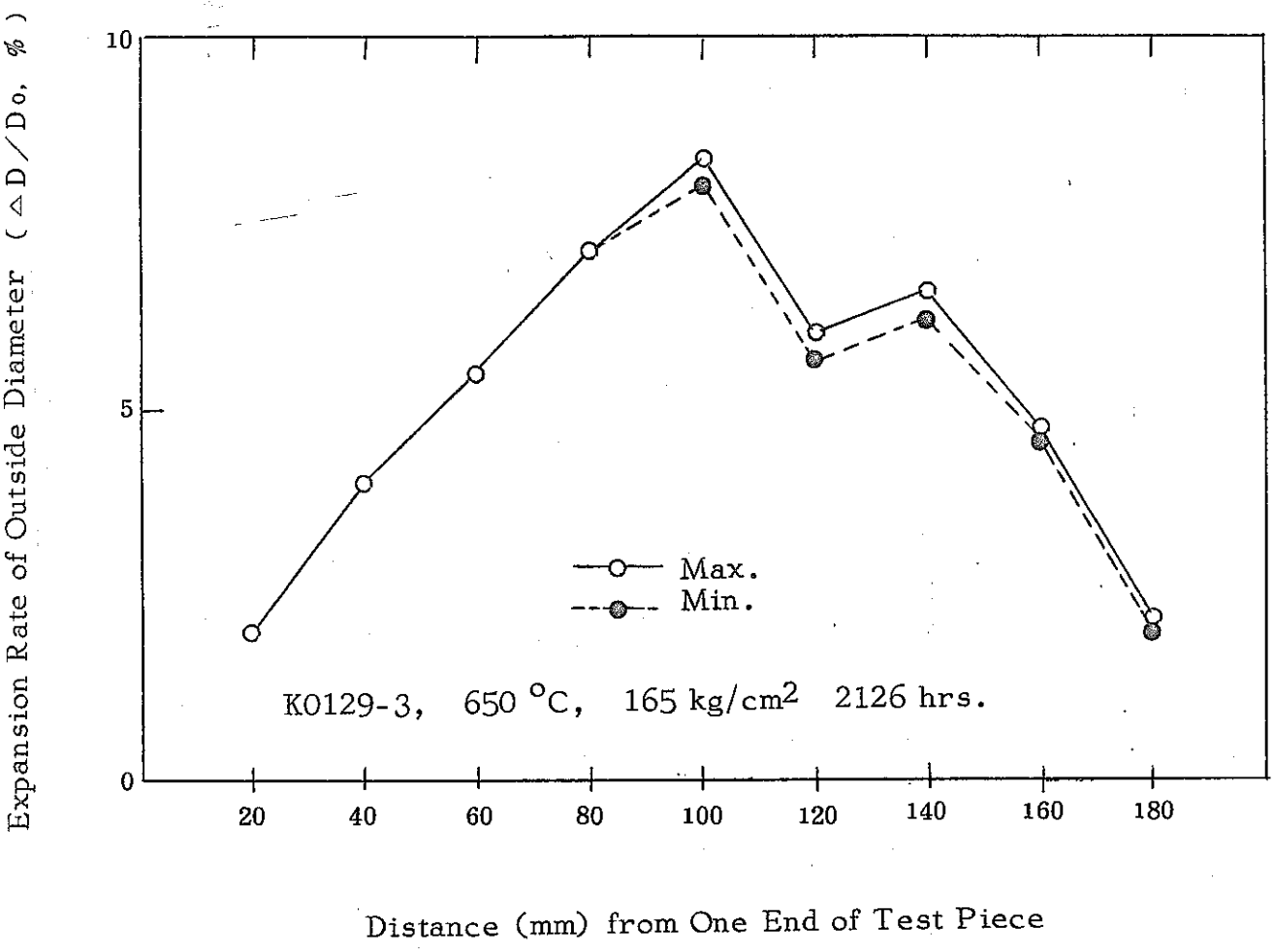

Fig. 15. Expansion Rate of Outside Diameter of Test Pieces after Rupture

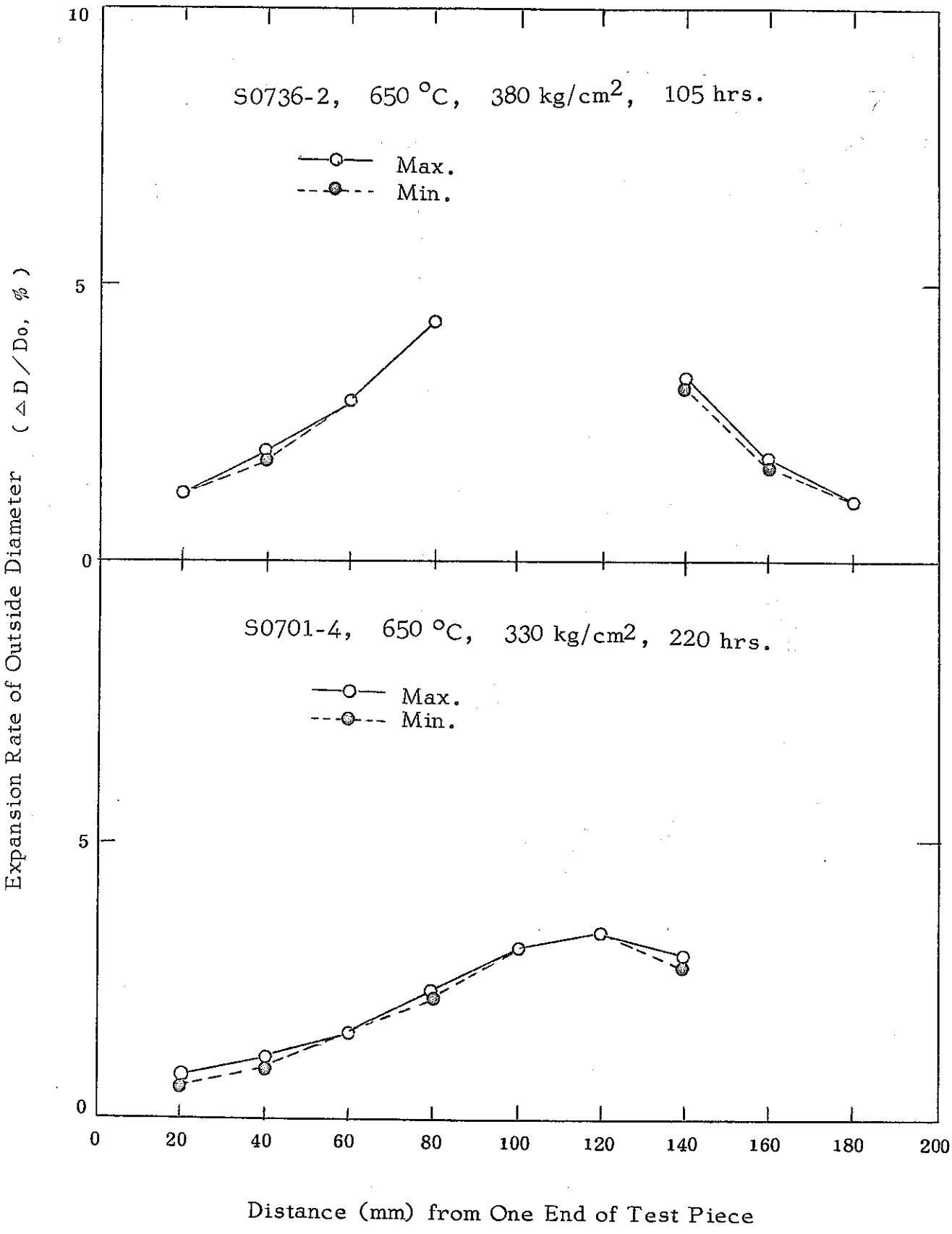

Fig. 16. Expansion Rate of Outside Diameter of Test Pieces after Rupture

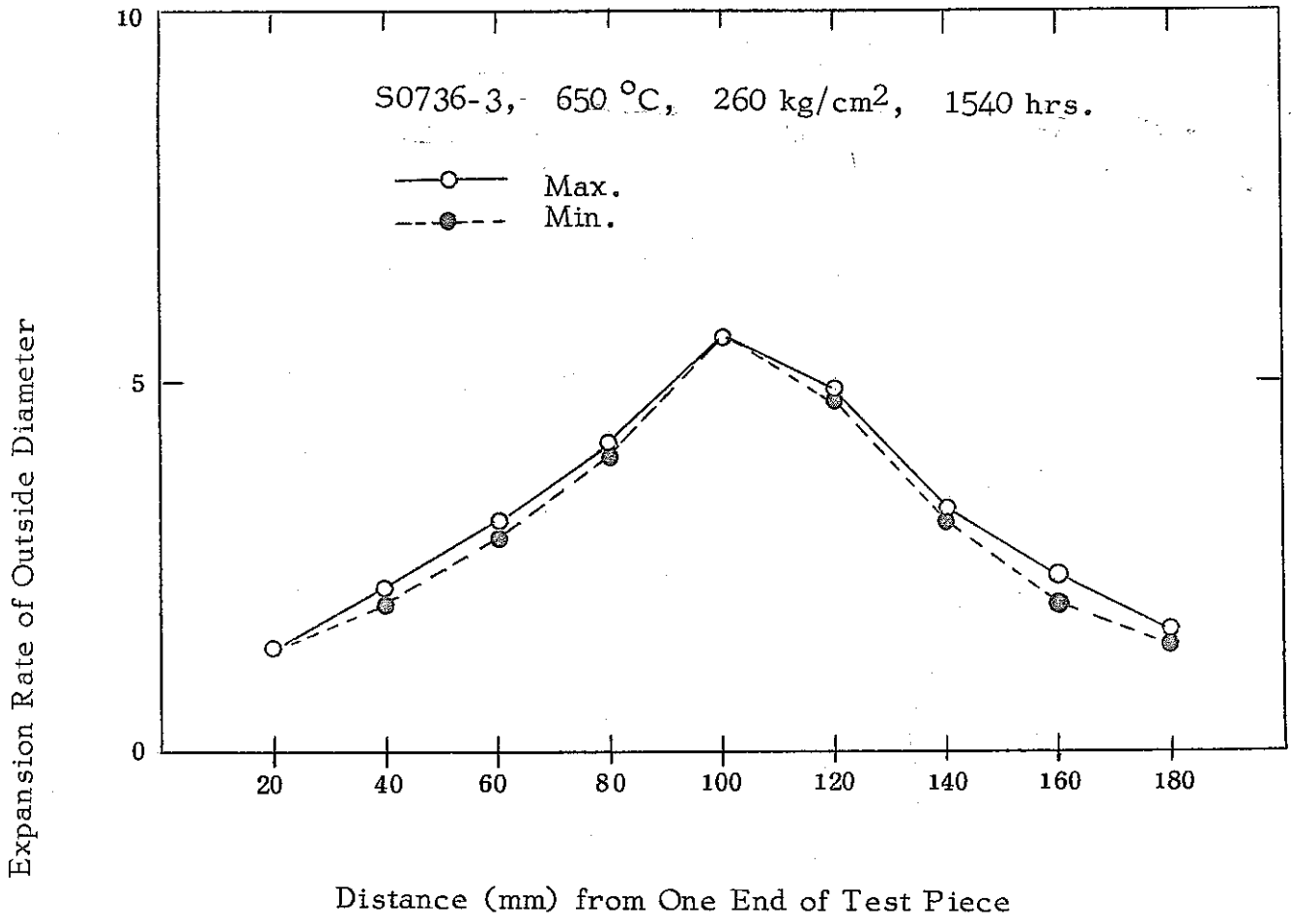

Fig. 17. Expansion Rate of Outside Diameter of Test Pieces after Rupture

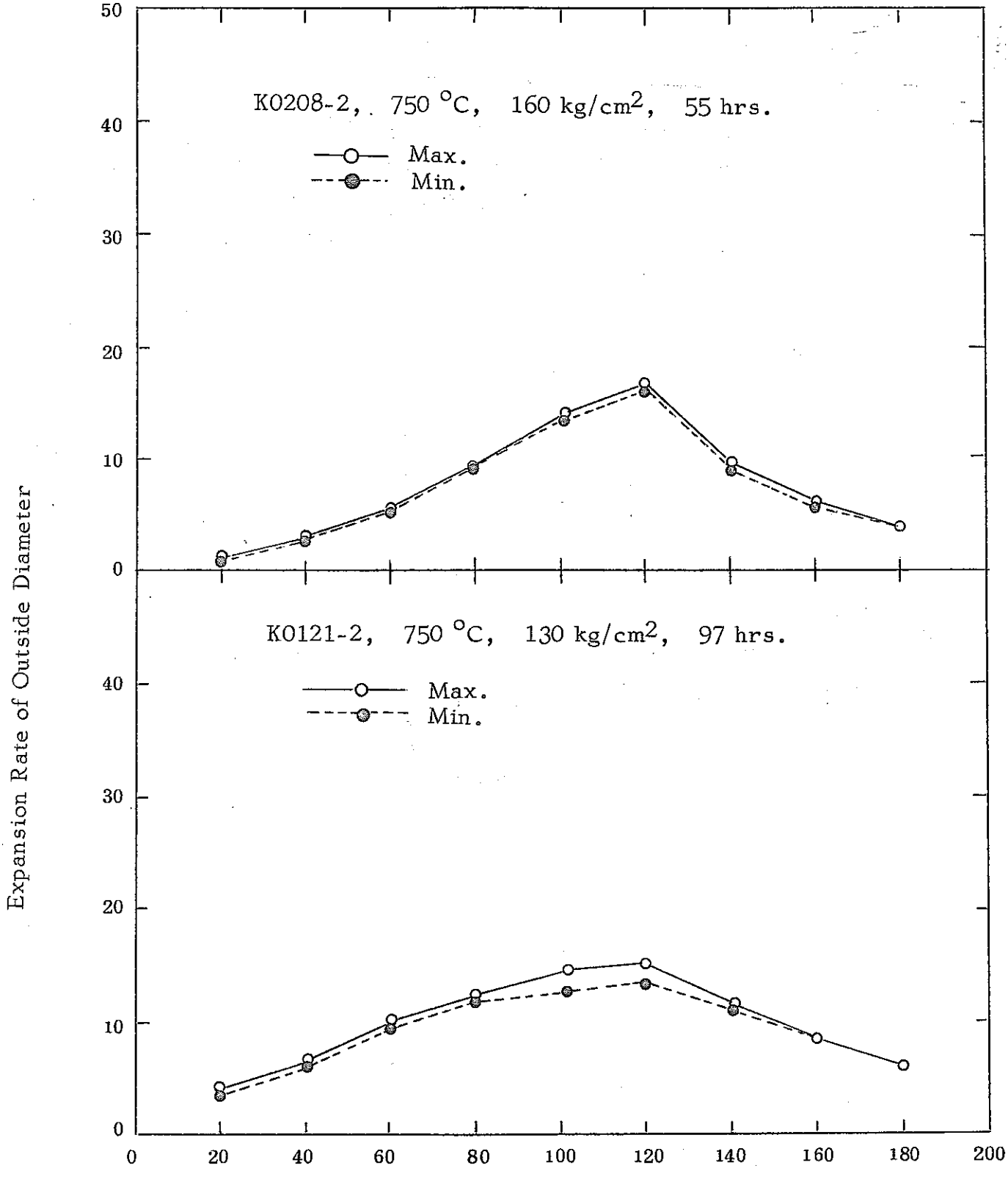

Fig. 18. Expansion Rate of Outside Diameter of Test Pieces after Rupture

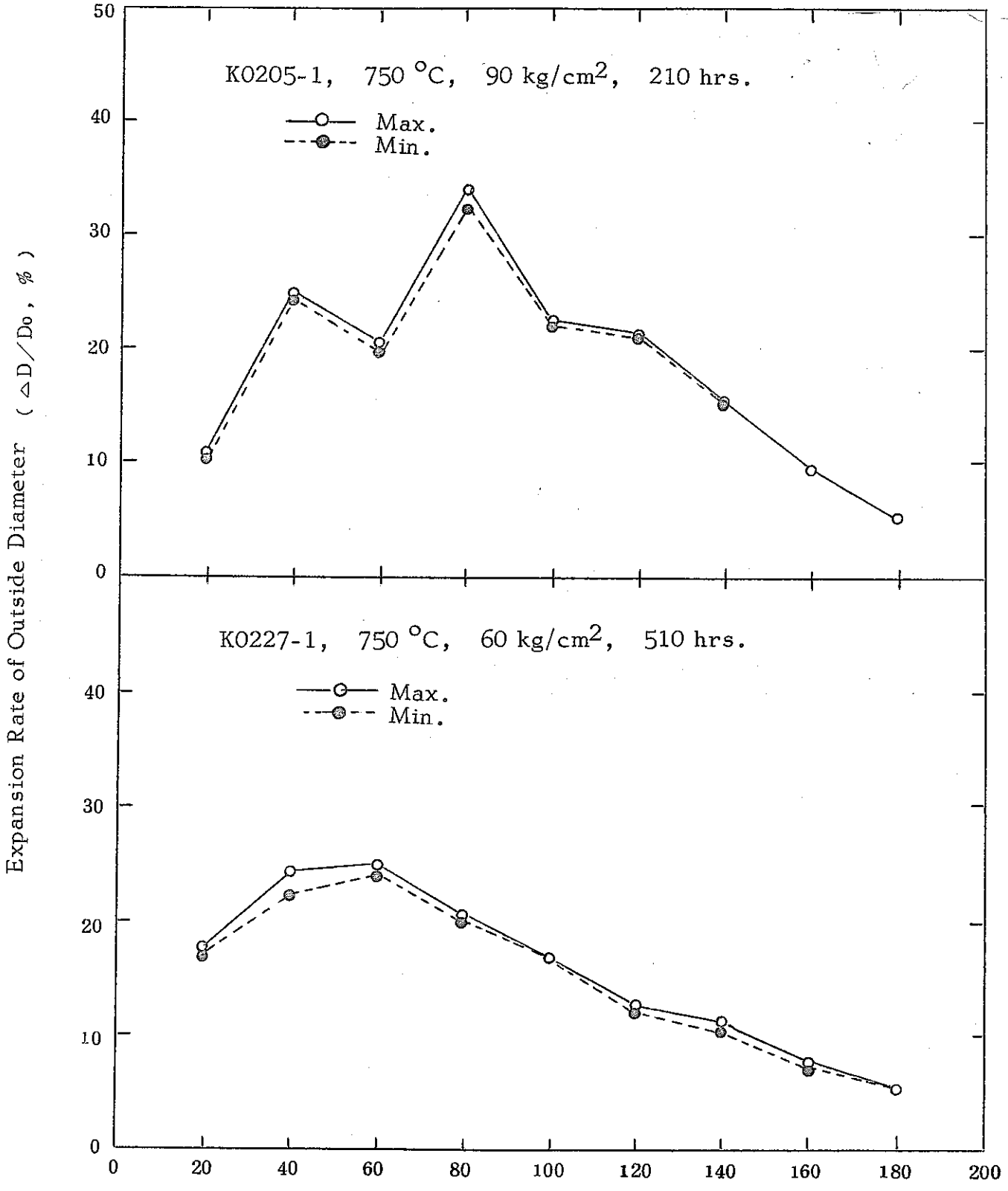

Fig. 19. Expansion Rate of Outside Diameter of Test Pieces after Rupture

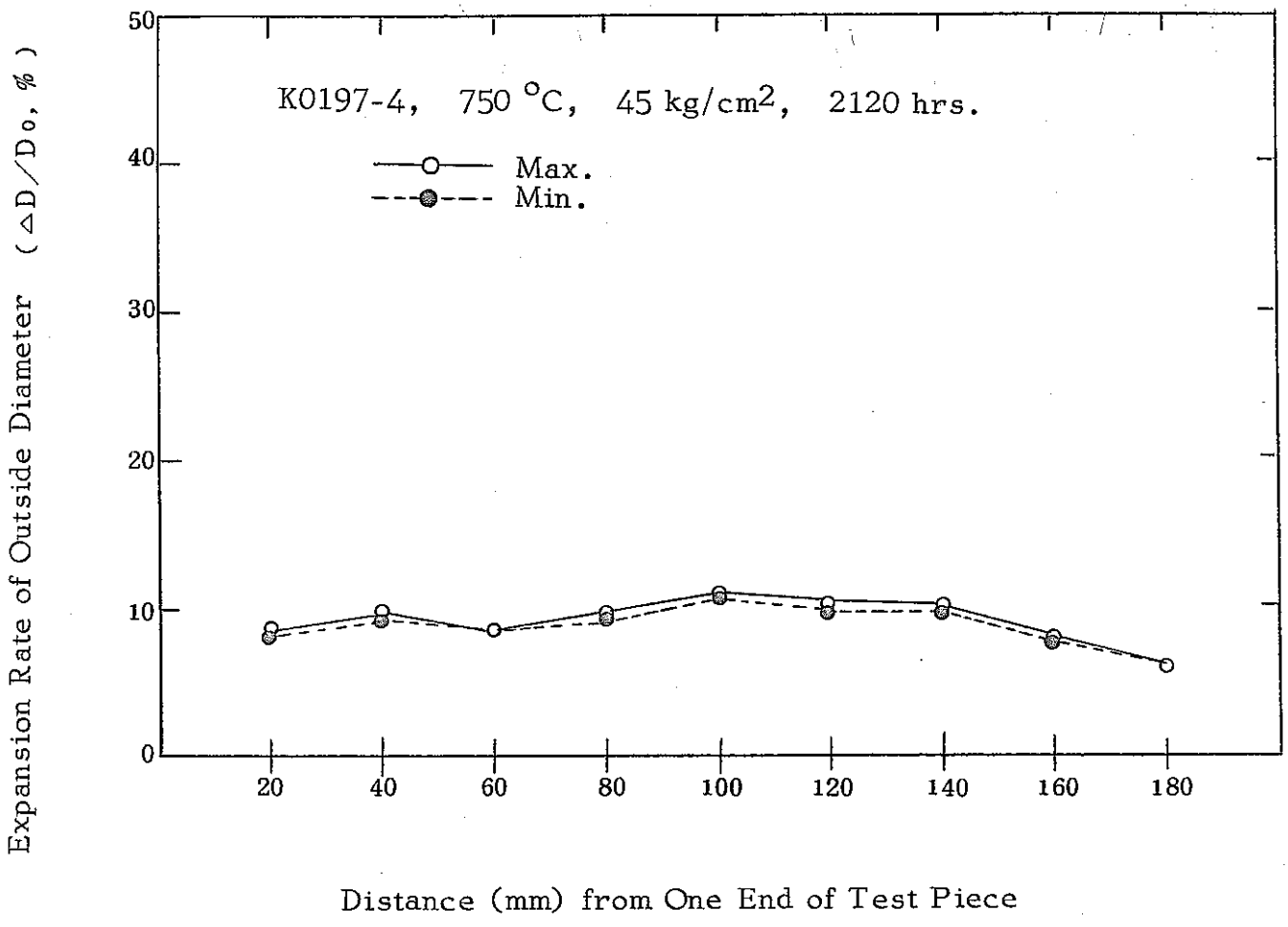

Fig. 20. Expansion Rate of Outside Diameter of Test Pieces after Rupture

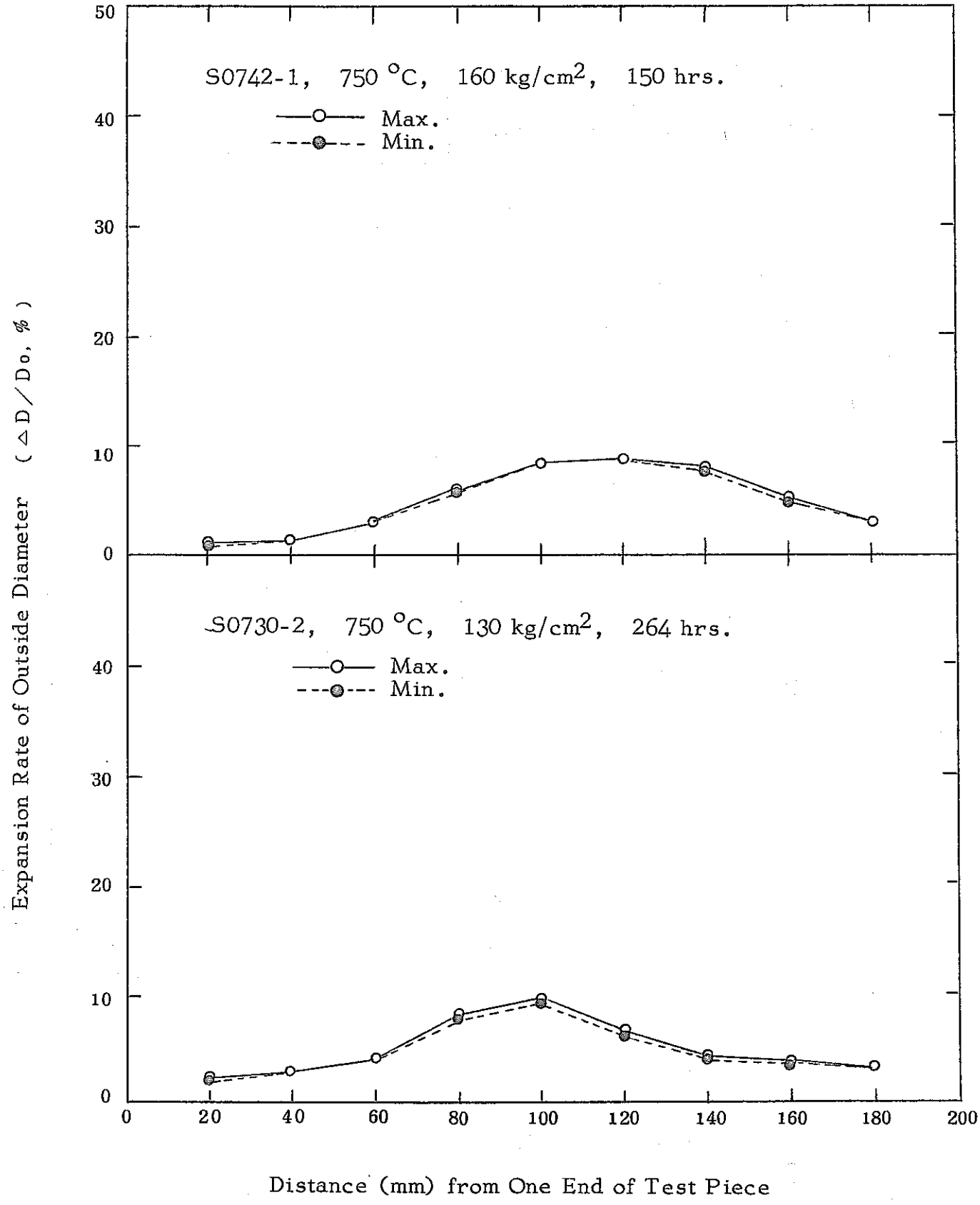

Fig. 21. Expansion Rate of Outside Diameter of Test Pieces after Rupture

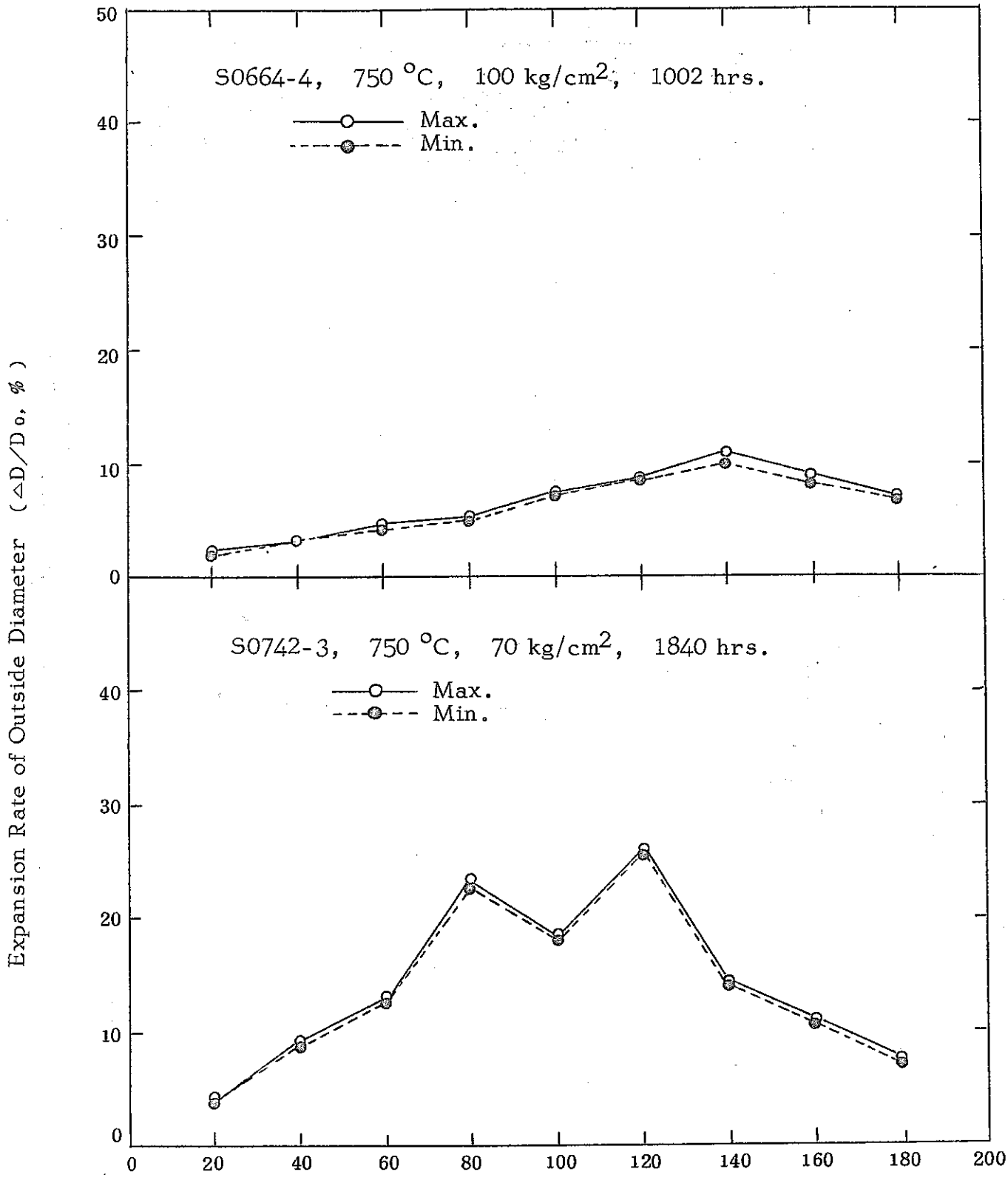

Fig. 22. Expansion Rate of Outside Diameter of Test Pieces after Rupture

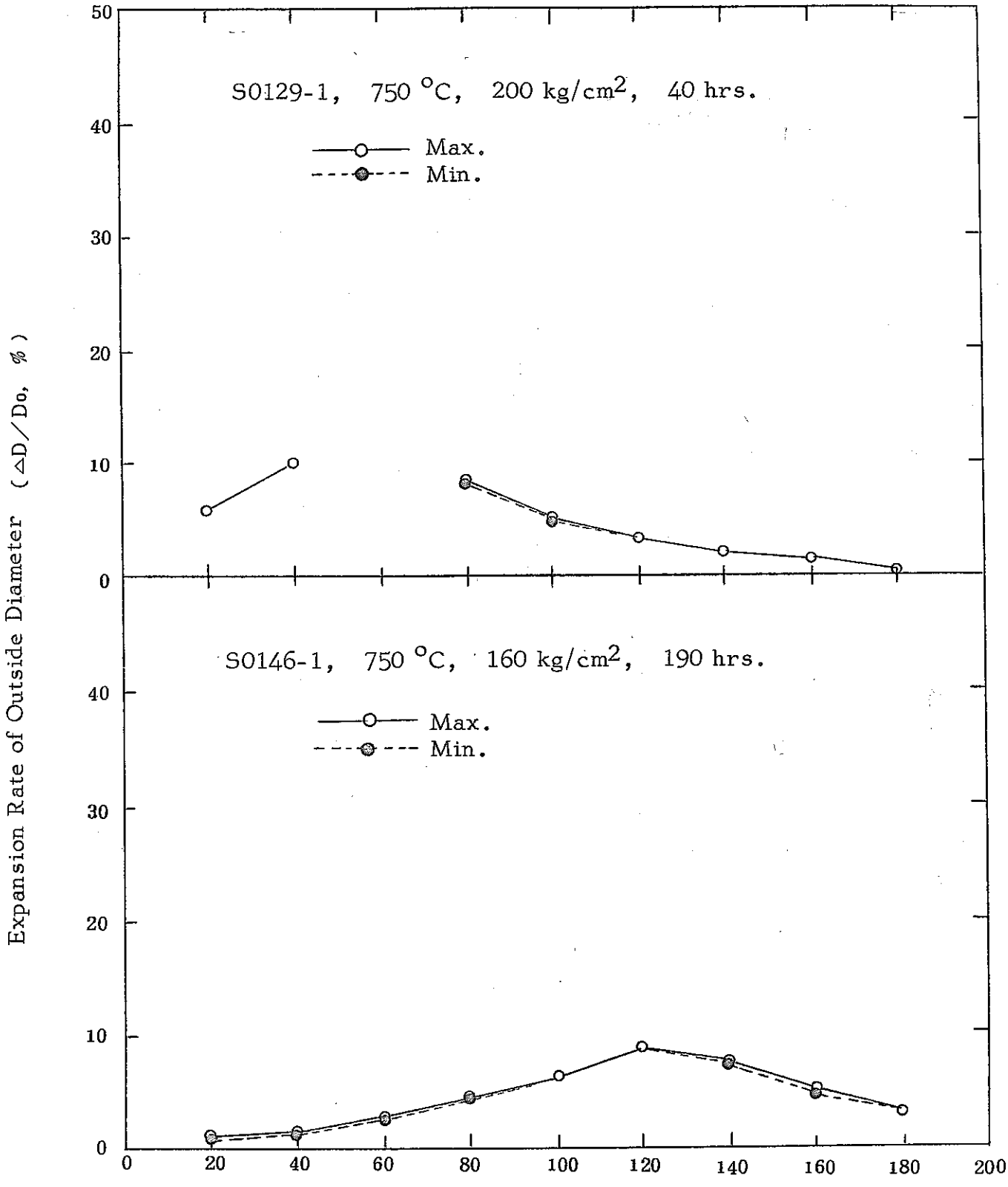

Fig. 23. Expansion Rate of Outside Diameter of Test Pieces after Rupture

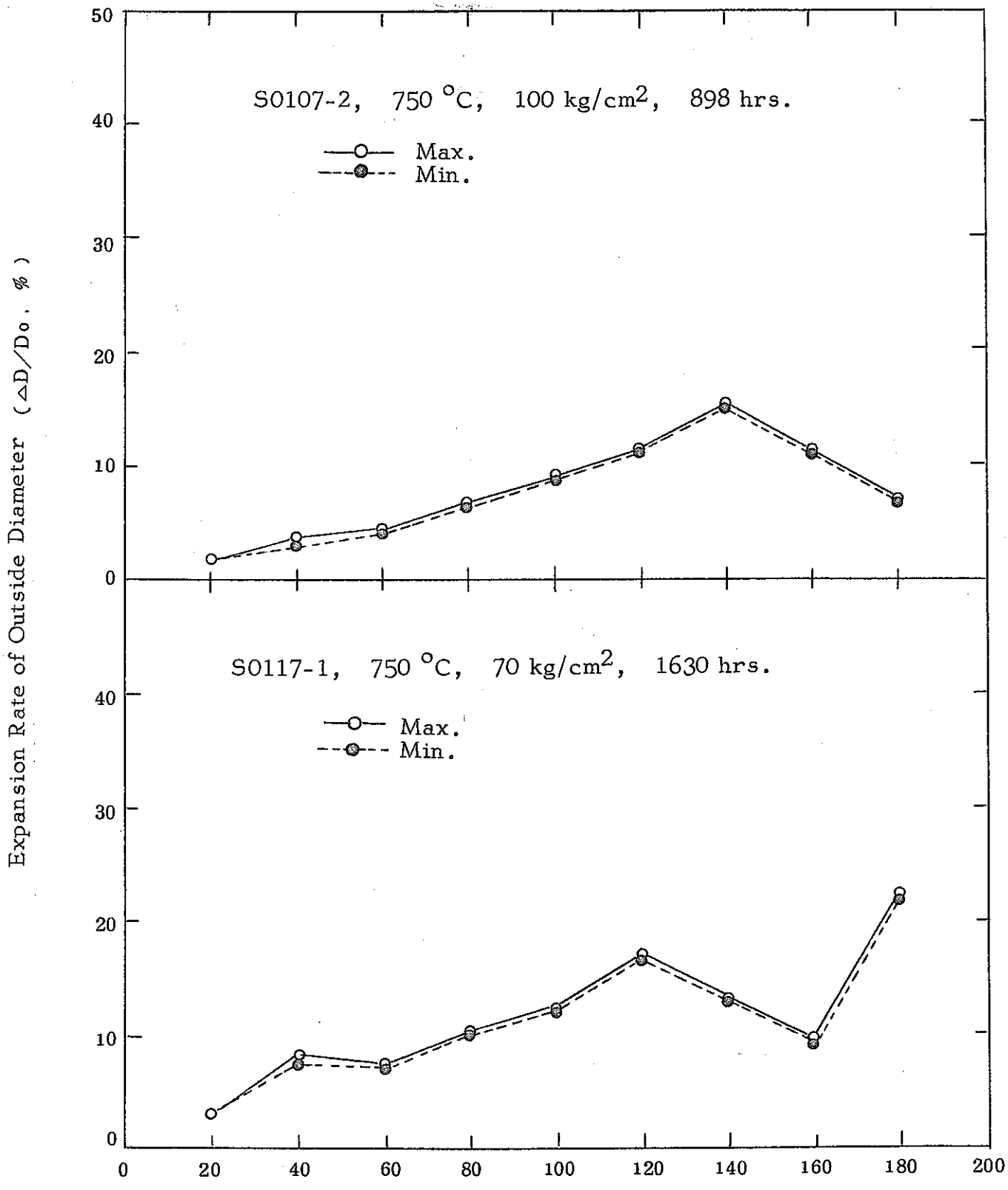

Fig. 24. Expansion Rate of Outside Diameter of Test Pieces after Rupture

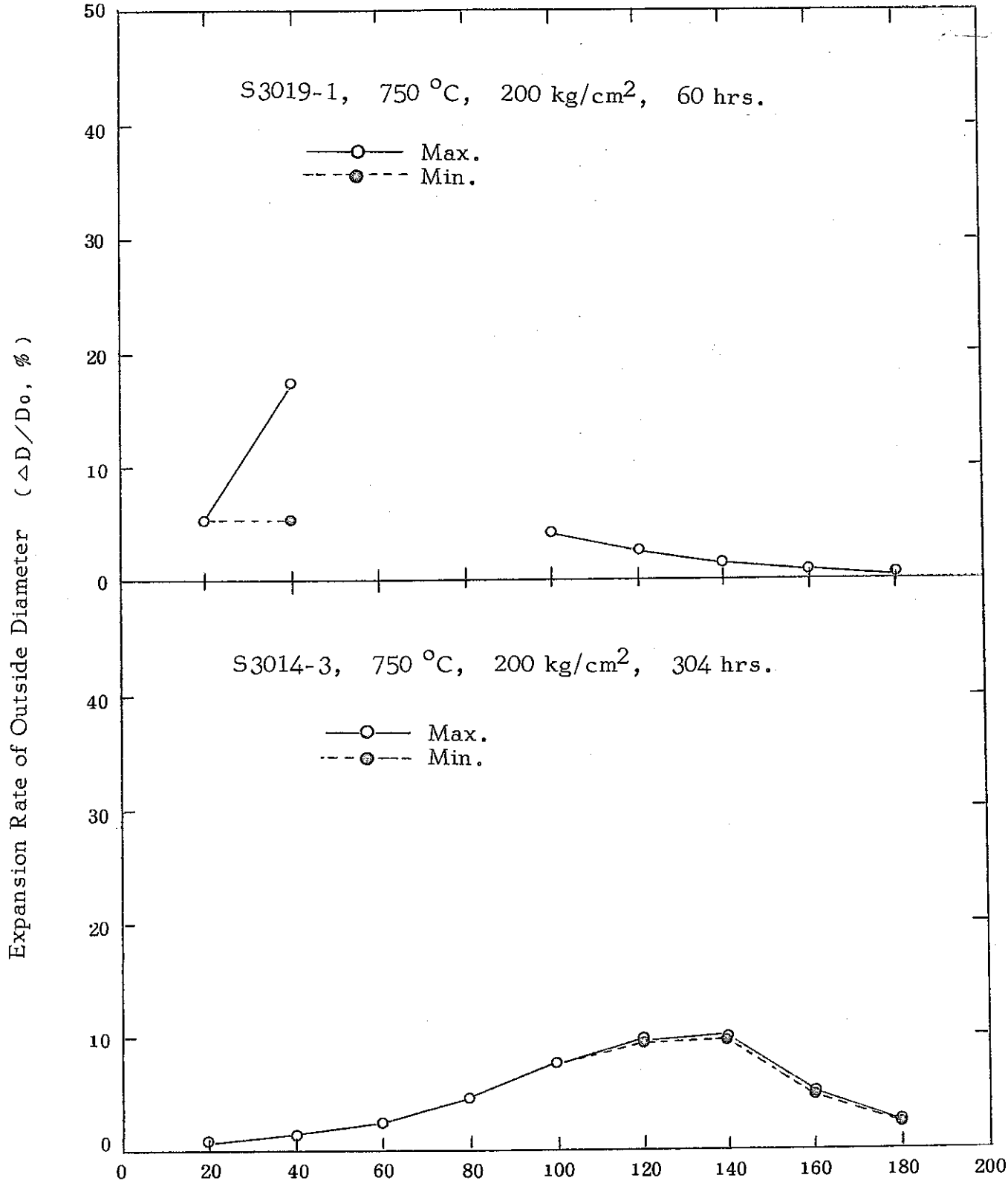

Fig. 25. Expansion Rate of Outside Diameter of Test Pieces after Rupture

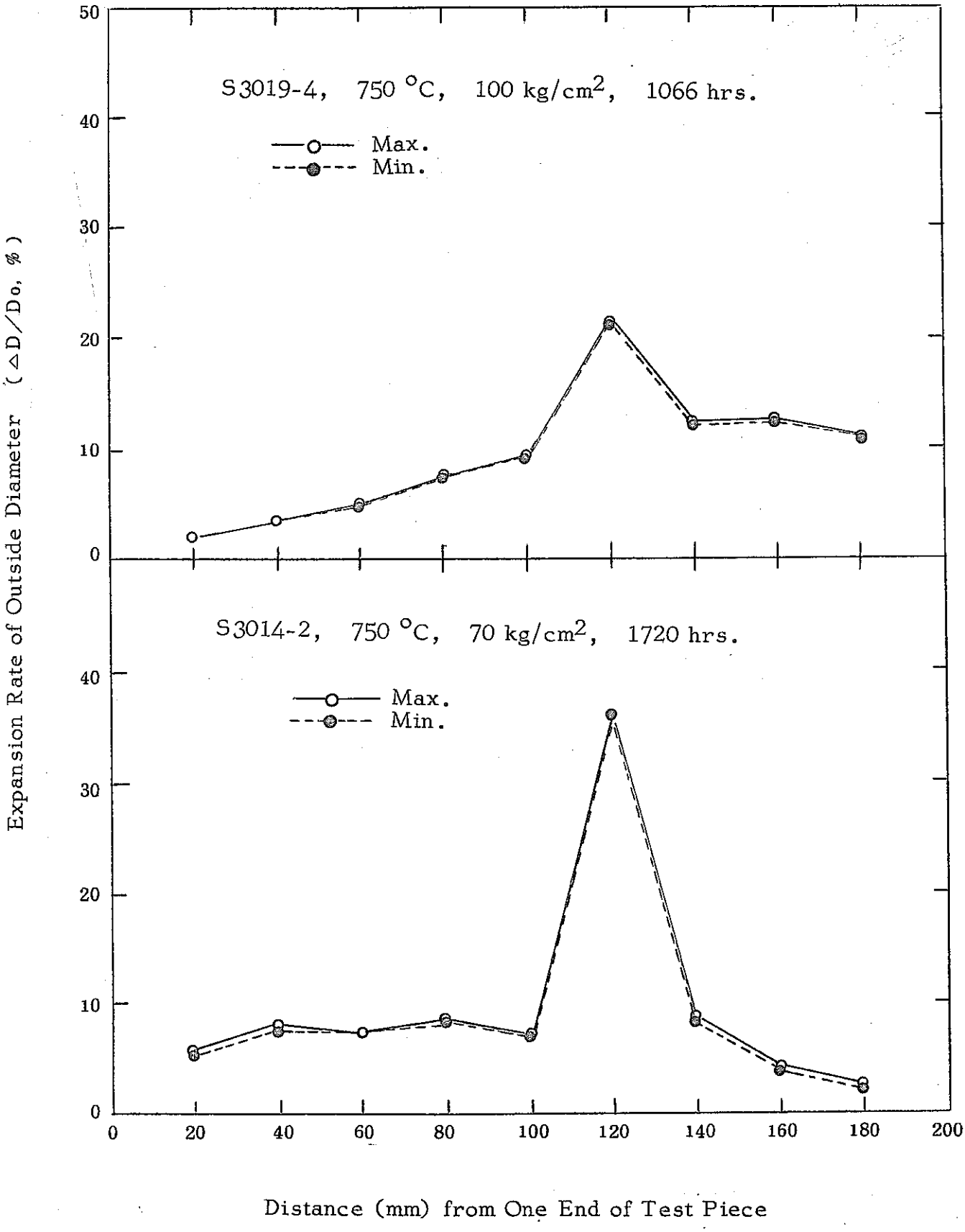

Fig. 26. Expansion Rate of Outside Diameter of Test Pieces after Rupture

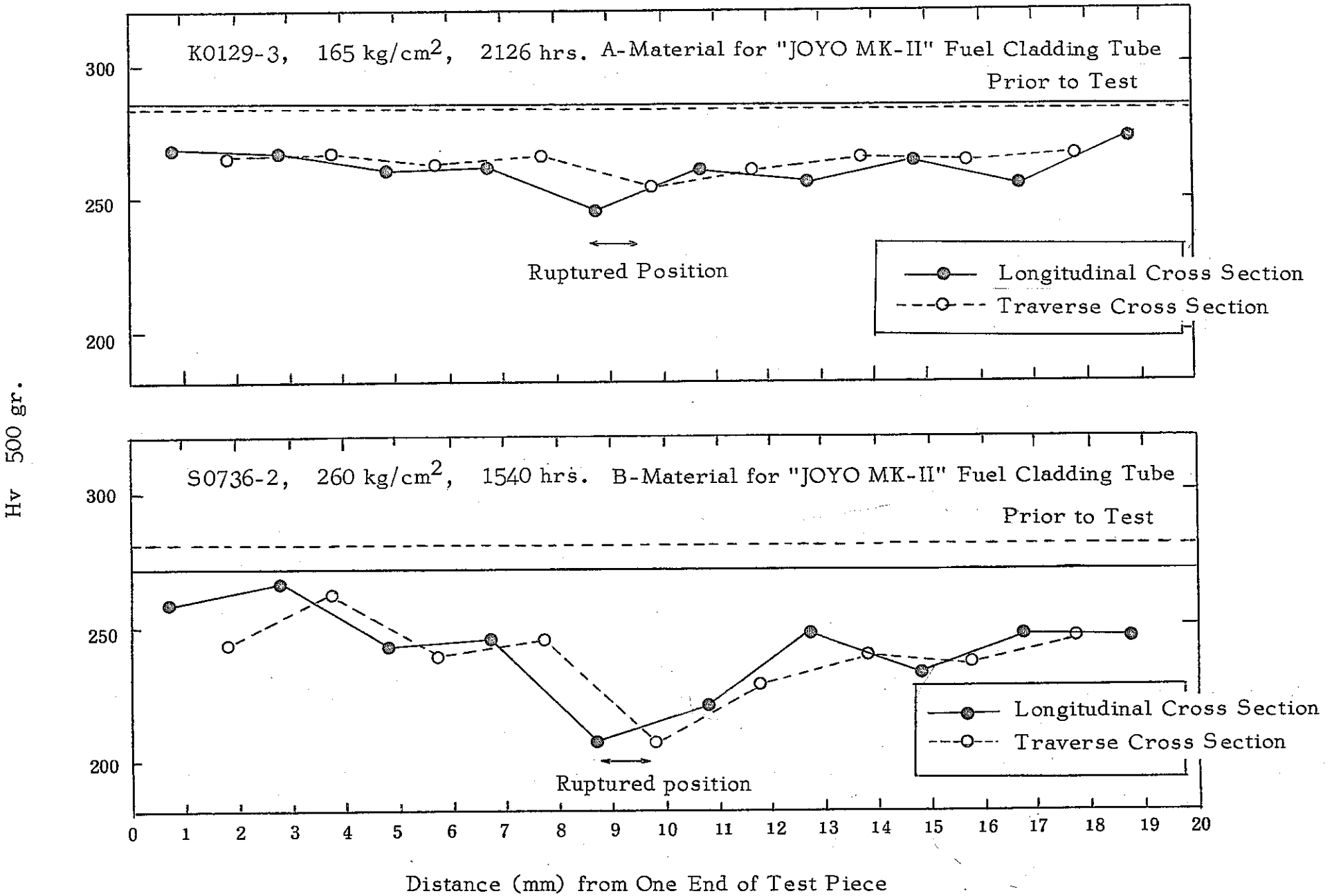

Fig. 27. Hardness Distribution after Long-Time Endurance Test at 650 °C

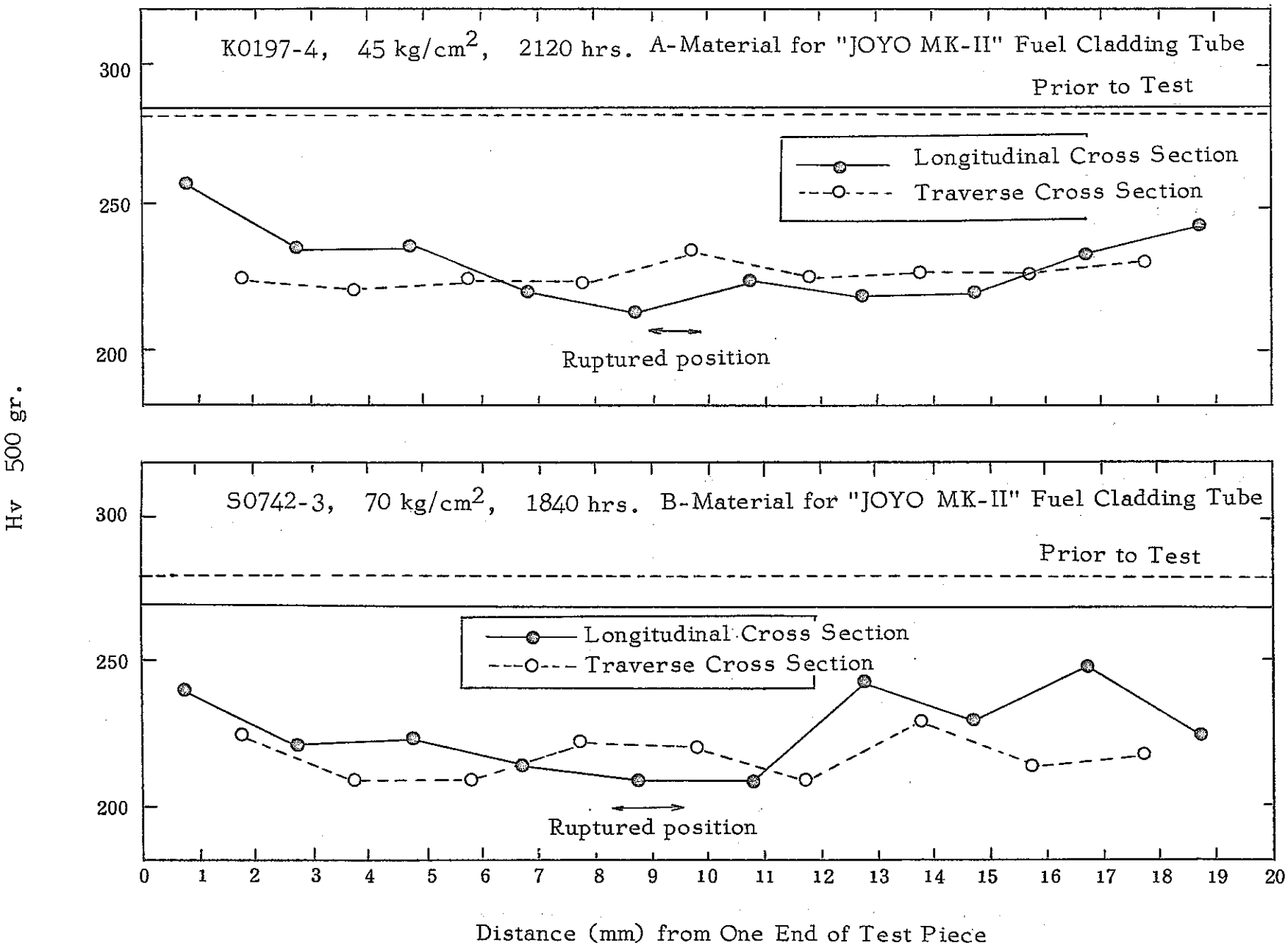

Fig. 28. Hardness Distribution after Long-Time Endurance Test at 750 °C

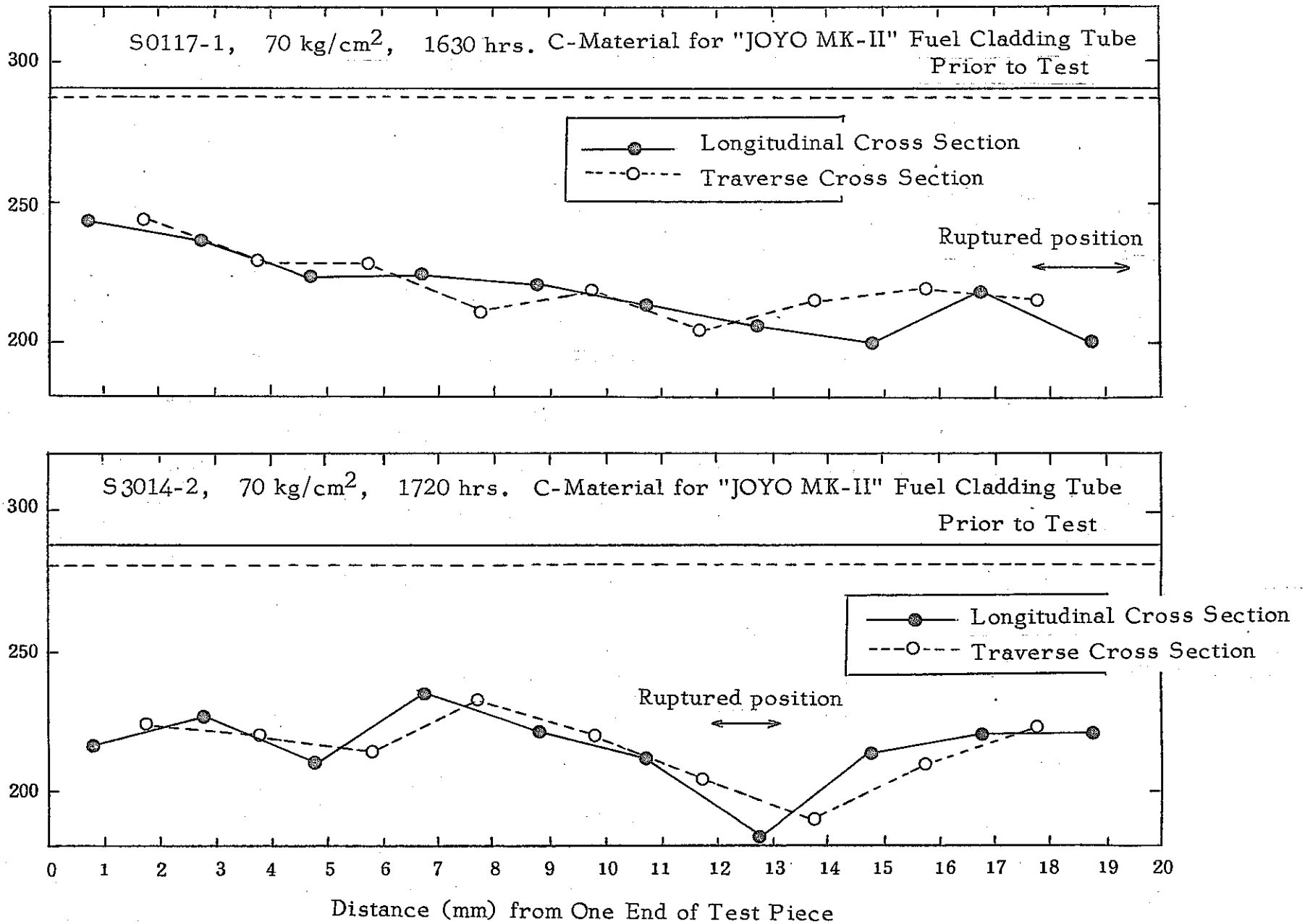

Fig. 29. Hardness Distribution after Long-Time Endurance Test at 750 °C

5. Conclusion

A series of high temperature tensile tests and uniaxial creep tests were undertaken on the 2nd trial-made materials of A and B for "MONJU" fuel cladding tube, and also a series of internal pressure creep rupture tests were performed on the materials of A, B and C, for "JOYO" fuel cladding tube, and on the material C for "MONJU" fuel cladding tube. Through these tests, the high temperature strength of these materials for fuel cladding tubes for both kinds of reactor cores have been elucidated.